University of Zurich UZH

Soil organic carbon vulnerability in Swiss alpine soils: The effect of elevation and parent material on carbon pools and fluxes

GEO 511 Master's Thesis

Author
Cédric Bührer
18-739-698

26.04.2024
Department of Geography, University of Zurich

Abstract

Climate change potentially impacts soil organic matter [SOM] in alpine soils by accelerating decomposition and altering carbon [C] inputs into soils due to upward shifts in vegetation. The direction and magnitude of soil organic carbon [SOC] changes are still uncertain and the impact of parent material on SOC stability has rarely been assessed. Here, soil respiration [SR] was measured during the vegetation period of 2023 along three elevational gradients with different parent material (gneissic, amphibolitic, and calcareous) ranging from 1750 to 3100 m near Davos, Switzerland. A physical particle size fractionation of topsoil samples (0 -10 cm) was conducted to evaluate labile and stable soil organic matter [SOM]. The results indicate that topsoil bulk SOC stocks increase with decreasing elevation possibly related to an enhanced input of C by an increasing vegetation productivity. While SOC stocks in the "labile" coarse particulate organic matter [cPOM] decrease significantly with increasing elevation, the two other fractions do not show a linear pattern with elevation. However, stocks of "stable" mineral-associated organic carbon [MAOC] are greatest on grassland sites probably due to an enhanced productivity of fine roots and the abundance of microbial necromass in these topsoils. Soil respiration increases with decreasing elevation likely due to an increase in temperature, vegetation productivity, and higher SOC stocks.

On average, SR is more than twice as high on calcareous compared to siliceous parent material likely due to the consistently higher pH of calcareous topsoils which promotes microbial activity. There are no significant differences between parent materials for bulk SOC stocks and C pools within the soil fractions in the topsoil. However, grassland topsoils between 2000 and 2500 m on gneissic parent material have the highest bulk SOC and MAOC stocks. While elevational trends of C fluxes and stocks could be confirmed, the impact of parent material remains partially uncertain. Therefore, it is crucial for future studies to consider bulk SOC stocks, labile, and stable SOM fractions of entire soil profiles to make more accurate predictions about how the parent material affects the vulnerability of SOC under future climate change.

Acknowledgments

Contents

Abbreviations

C	Carbon
CO_2	Carbon dioxide
cPOM	Coarse particulate organic matter
cPOC	Coarse particulate organic carbon
DR	Dischmatal – Fuorcla Radönt (Transect 3)
FS	Flüelapass – Schwarzhorn (Transect 2)
fPOM	Fine particulate organic matter
fPOC	Fine particulate organic carbon
IB	Inneralpen – Büelenhorn (Transect 1)
IPCC	Intergovernmental Panel on Climate Change
MAOM	Mineral-associated organic matter
MAOC	Mineral-associated organic carbon
N	Nitrogen
POM	Particulate organic matter
POC	Particulate organic carbon
Q_{10}	Temperature sensitivity
SLF	Institute for Snow and Avalanche Research
SOC	Soil organic carbon
SR	Soil respiration
SR_{10}	Standardized soil respiration at 10°C
T1/2/3	Transect 1, 2 or 3
WSL	Swiss Federal Institute for Forest, Snow and Landscape Research
XThaw	Project ExtremeThaw

1 Introduction

1.1 Background & Motivation

Soils form the interface between hydrosphere, biosphere, geosphere, and atmosphere and are influenced by abiotic as well as biotic factors (Hagedorn et al., 2018): They are the product of a wide variety of factors such as climatic variables, time, topography, parent material, flora, and fauna (Egli & Poulenard, 2016). In the terrestrial biosphere, soils contain the largest reservoir of carbon [C], storing about 1400 Gt of soil organic carbon [SOC] (Green & Byrne, 2004). This is about three times more organic C than the worlds biomass and three times more than the atmosphere contains in carbon dioxide [CO_2] alone (Intergovernmental Panel on Climate Change [IPCC], 2007). With such an immense reservoir size, soils take in an important spot in the terrestrial carbon cycle (Gubler et al., 2022).

The C cycle in soils is controlled by three main factors: Climatic variables (e.g. precipitation and temperature) (Sanderman et al., 2003), the composition and storage of C as well as decomposition rates (Gleixner et al., 2001), and any removal or addition of C into the cycle (Krull et al., 2003, Zollinger et al., 2013).

Soils constantly exchange C in that cycle. Carbon can enter the soil through decaying organic material, root, and animal excretions (Gubler et al., 2022). A small amount of it is then transformed and decomposed by soil animals and microorganisms which turn it into soil organic matter [SOM] (Hagedorn et al., 2022). SOM is a heterogeneous mix of organic material with variable degrees of decomposition (Hitz et al., 2001). About half of it consists of C which is then called soil organic carbon [SOC] (Hagedorn et al., 2022). It makes up for about two thirds of global soil bound C while the remainder is held as inorganic C (Batjes, 1996, Scharlemann et al., 2014).

The quality of SOC, describing its resistance to decomposition, may ultimately be related to the form of SOM in which it is stored (Lugato et al., 2021): In general, two functionally different fractions can be distinguished (Lavallee et al., 2020): Particulate organic matter [POM] consists of structural polymeric organic compounds with a relatively short lifespan (residence time between years to decades) (von Lützow et al, 2007). Those compounds are at an early stage of decomposition and are usually not protected in aggregates (von Lützow et al, 2007). Due to its high accessibility, POM is not well protected from microbial decomposition in the long-term. Furthermore, POM is highly vulnerable to environmental changes due to its reliance on microbial inhibition (Dutta & Dutta, 2016; Lugato et al., 2021).

On the contrary, mineral-associated organic matter [MAOM] is made of molecular weight compounds which have been formed by microbial processing of organic material (Cotrufo et al., 2019). MAOM is protected from quick decomposition due to its association with mineral surfaces (e.g. derived from weathering processes) which leads to a longer lifespan in the soil (residence time between decades to

centuries) (von Lützow et al, 2007). Therefore, it is expected to be less vulnerable to disturbances and environmental changes as POM (Rocci et al., 2020, Lugato et al., 2021).

In the end, only a small percentage of SOC is stored permanently, and large parts of C are also released back to the atmosphere as CO_2 through mineralization of SOC (or methane under anaerobic conditions) (Hagedorn et al., 2010b, Hagedorn et al., 2022).

The release of SOC through root and microbial respiration is called soil respiration [SR] (Gubler et al., 2022). It alone is responsible for unlocking of up to 79.3–81.8 Pg C yr^{-1} globally to the atmosphere (Schlesinger & Andrews, 2000; Rodeghiero et al., 2005). On earth, about 10% of the atmosphere's CO_2 circulates through soils each year (Rodeghiero et al. 2005). This exchange in CO_2 is about ten times bigger than the release of CO_2 from fossil fuels (Hagedorn et al., 2010b). After photosynthesis, it is the largest biological C flux in terrestrial ecosystems (Luo et al., 2001, Badraghi et al., 2021).

About as much C is absorbed by soils globally as is released through SR under stable conditions and climate (Hagedorn et al., 2010b). However, the IPCC (2023) states in its latest report, that global surface temperatures have reached 1.1°C above pre-industrial levels (1850 – 1900) due to the release of fossil CO_2 (and other greenhouse gases) to the atmosphere. This has led to changes in the world's climate system and directly influences the world's soils (IPCC, 2023). Hence, if environmental changes affect the fate of soil C, it may have a direct impact on the atmospheric CO_2 concentration (Rodeghiero et al. 2005).

In stark contrast to lowland soils, on which the impact of climatic changes has already been studied intensively (Trautmann et al., 2023), there is still a lack of data on how soils in higher elevations react to changing conditions (Gubler et al., 2022).

Mountain environments make up for 12% of the world's terrestrial surface (Körner, 2003) resp. 3% of Europe's continent (Gubler et al., 2022) and provide a wide variety of crucial ecosystem services such as C storage and water reservoirs and are hotspots of biodiversity (Körner, 2003). Soils in alpine areas worldwide have average SOC stocks of 15.2 ± 1.3 kg C m^{-2} which is about the same as temperate grasslands (Bockheim & Munroe, 2014) and more than average global SOC stocks (approximately 8.2 to 10.6 kg C m^{-2} within the first 100cm of soil depth) (Eswaran et al., 1993; Jobbagy & Jackson, 2000). Although the snow-free vegetation period is short and biomass inputs are thus relatively low, SOM accumulation can outweigh SOM degradation in the long term (Gavazov et al., 2017). In high elevations, the decomposition of SOM is usually low because of the lowered biological and chemical mineralization rates under colder climatic conditions (Schimel et al., 1994; Djukic et al., 2010; Trautmann et al., 2023). Those hostile climatic conditions favor the storage of SOC in alpine soils and have led to considerable C stocks, even though alpine soils are usually only a few decimeters or even centimeters thick (Trautmann et al., 2023).

These C stocks are now under threat (Pintaldi et al., 2021) as the European Alps experience strongly changing precipitation conditions and are warming more than the global average (Rebetez and Reinhard, 2008; Gobiet et al., 2014). They currently face the strongest climatic warming over the last few thousand years (Hagedorn et al., 2010b).

In the Swiss Alps, mean annual temperatures have risen by 0.57 °C per decade while the increase in the northern hemisphere is "only" about 0.25 °C per decade (Hagedorn et al., 2010a). Climate change may therefore raise soil temperature that will directly influence soil parameters (Hitz et al., 2001; Pepin et al., 2015). Hence, the altering conditions in higher elevations will ultimately affect the dynamics of alpine soils and its C stocks (Bockheim & Munroe, 2014; Pintaldi et al., 2021). Moreover, Hitz et al., (2001) state that mountainous ecosystems are highly responsive to climatic changes which may promote plant migration due to the sharp vegetation gradients present in alpine regions, change plant productivity, and shorten the duration of snow cover. Rumpf et al. (2022: p. 1119) concluded that "*77% of the European Alps above the tree line experienced greening (productivity gain)*" and although not equally strong everywhere, *"snow cover declined significantly during this time"*.

1.2   Knowledge gaps

SOC dynamics at higher elevations have increasingly moved to the center of research in recent decades, because any additional in- or decrease in SOC may be relevant for the future course of climate change (Gubler et al., 2022). In this field of research, particular attention was paid to C stocks, the vulnerability of SOC to changing climate conditions, and how SR is being influenced by biotic and abiotic factors (Zollinger et al., 2013; Badraghi et al., 2021).

Gradient studies have been proven to be particularly useful in this context as they offer the opportunity to investigate SOC development under different climatic factors along a gradient with otherwise rather similar environments (Leifeld et al., 2009). Changes in the belowground system can be documented (Hagedorn et al., 2019) and an elevational gradient reflects factors that are likely to change with climate change (Hagedorn et al., 2010b). Therefore, such studies promote our understanding of a changing world at higher elevations (Leifeld et al., 2009).

Among other studies, Guo et al. (2022) found SR to increase with decreasing elevation. This may be connected to higher plant productivity and warmer temperatures in lower elevations (Badraghi et al., 2021; Guelland et al., 2013). However, a higher input of C into the soil may also lead to higher stocks of SOC in lower elevations than in high elevated sites (Zollinger et al., 2013). Hence, an increased litter production can increase SOC stocks and therefore lead to enhanced SR rates (Badraghi et al., 2021). On the contrary, Sjögersten et al. (2003) and Leifeld et al., (2009) looked at the stability of SOM and reported higher proportions of POM with increasing elevation along elevational gradients which correlated positively with SR. This is also supported by the findings of Hagedorn & Joos (2014). Therefore, quantity and quality of SOC seem to be important to in predicting SR in alpine gradients.

Research in alpine environments on SR and SOC also focused on a set of drivers which would impact these factors. Here, soil temperature and soil moisture are viewed as the major abiotic factors to control the release of SOC through SR (Fang & Moncrieff, 2001; Zhao et al., 2017). Moreover, soil parameters such as pH, C/N, texture, bulk density, and nutrients as well as vegetation, geomorphology, precipitation, climate and mean residence time of SOM influence the fate of SOC and thus SR (Budge et al., 2011; Bird et al., 2001; Badraghi et al., 2021; Pan et al., 2024).

Still, most studies only investigated a certain number of parameters in alpine environments and explicitly tried to exclude others in order to minimize their influence as far as possible. This also includes, among other factors, the parent material, which they tried to exclude by conducting the studies on only one slope of the same parent material in each case. This enabled them to rule out any possible influences of the parent rock on SR, SOC stock or the stability of the SOM (e.g. Rodeghiero et al. 2005; Leifeld et al., 2009; Djukic et al., 2010; Budge et al., 2011; Badraghi et al., 2021).

However, parent material plays an important role in soil formation and thus influences soil parameters as well as above ground processes (Egli & Poulenard, 2016; Simon et al., 2020). Zhang et al. (2022) concluded that total SOC stocks varied considerably across different parent materials in south-western China. And a study conducted in alpine meadows in Tibet found differences in SOC concentration of soil fractions to be significant between four different parent materials (Pan et al., 2024). Also, Angst et al. (2018) demonstrate in a study conducted in Germany that differences in parent material need to be considered to predict SOC stocks.

Musso et al. (2022) found soil production rates to differ considerably between siliceous and calcareous soils whereby the latter has a slower production rate due to slower weathering of calcareous parent material. Weathering of the parent rock is therefore decisive for the soil structure and properties such as SOC stock (Musso et al., 2022). Furthermore, Mikutta et al. (2009) argue that mineral weathering influences the proportion of labile and stable SOM. As parent material is increasingly weathered with soil age / decreasing elevation, the proportion of MAOM in soils is therefore expected to increase due to the association of SOM to mineral surfaces which enhances its stability (von Lützow et al, 2007; Mikutta et al., 2009). On the contrary, high mountain soils on poorly weathered rock can contain higher proportions of the rather labile POM stabilized through cold temperatures and thus slow litter decomposition and fewer soil organisms (Budge et al., 2011; Wackett et al., 2018; Hagedorn et al., 2019).

In the end, changes in alpine SOC storage are difficult to detect as they are quite small in relation to the total C stocks and usually occur only very slowly (Hagedorn et al., 2010b). Still, any additional in- or decrease in soil C may be relevant for the future course of climate warming (Gubler et al., 2022). Therefore, it is necessary to study which environmental factors influence SOC dynamics to better foresee the role of alpine soils as a C sink or source in the future (Zhao et al., 2017).

1.3 Research question

As the literature review has revealed contrasting results about SOC dynamics in higher elevations and only little data was available especially for the Swiss Alps (Hitz et al., 2001), this master's thesis tries to close knowledge gaps in a holistic approach by including the effects of different parent materials across vegetation zones: Along three elevational transects with different parent materials near Davos (Switzerland), SR has been measured alongside soil moisture and soil temperature during the vegetation period 2023. Besides field measurements and topsoil samples gathered during the field season 2023, the study has been enriched with already present data from the year 2022. Moreover, a physical particle size fractionation has been conducted with topsoil samples (0 – 10 cm) to assess the labile POM and stable MAOM fractions. Based on the existing research background, the following research questions and associated hypotheses were formulated:

How do soil organic carbon pools and fluxes change with elevation in alpine soils?

> **H1:** Bulk SOC stock increases with decreasing elevation due to higher C inputs of vegetation and stronger weathering of soils.

> **H2:** Contribution of MAOC to bulk SOC stock increases along elevational gradients with decreasing elevation due to increased weathering of the parent material.

> **H3:** Soil respiration increases with decreasing elevation through higher temperatures and increased input of C due to an increasing vegetation cover.

What is the influence of parent material?

> **H4:** Bulk SOC stock is higher on silicious than on calcareous parent material due to slower soil formation on calcareous parent material.

> **H5:** Parent material influences the SOC stability due to different weathering of parent materials with calcareous soils having less MAOC due to slower soil formation than siliceous soils.

> **H6:** Soil respiration is higher on calcareous parent material due to higher stocks of POC.

The study is embedded in the *ExtremeThaw* [XThaw] project, founded by the Extremes program at the *Swiss Federal Institute for Forest, Snow and Landscape Research* [WSL] and the *Institute for Snow and Avalanche Research* [SLF]. The aims of the project are to assess the potential impacts of thawing permafrost in high elevations such as the release of pollutants to alpine streams, pathogenic microorganisms to the environment, and ancient soil C. Furthermore, the capability of newly thawing soil to sequester C, harbor plants, and microbes is also being investigated (XThaw, 2022).

2 Study area

The research area of this thesis is situated in the Alps in the south-eastern part of Switzerland. More precisely, in the surrounding area of Davos in the canton of Grisons. It consists of three different transects which are located on three different parent materials. These transects contain a total of 28 sites ranging from 1750 to 3100 m and should allow to draw a comparison between montane to nival environments.

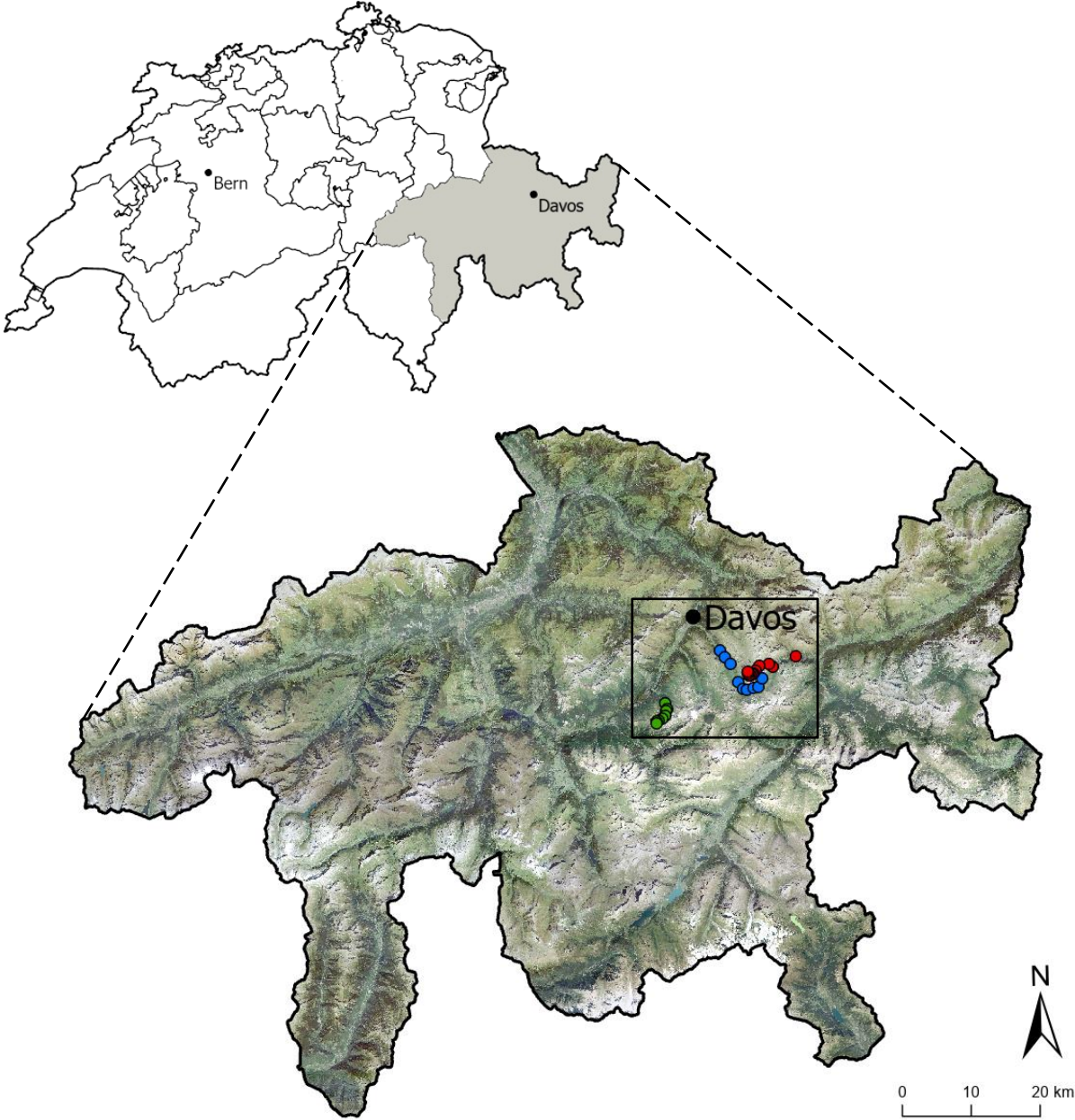*Figure 1: Localization of the study area (Swisstopo, 2024)*
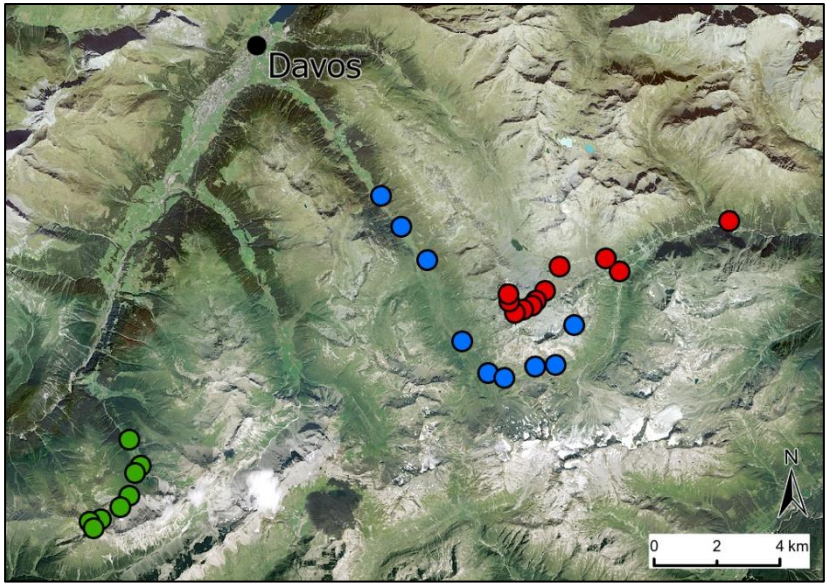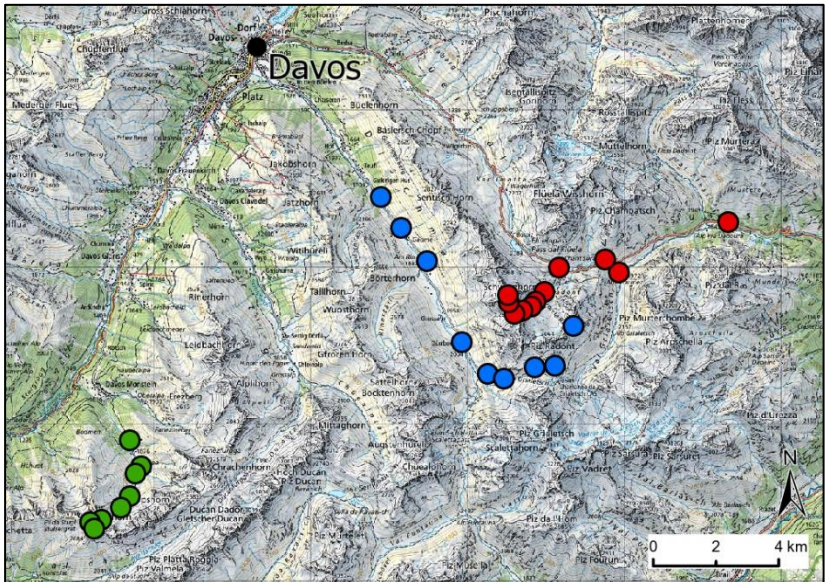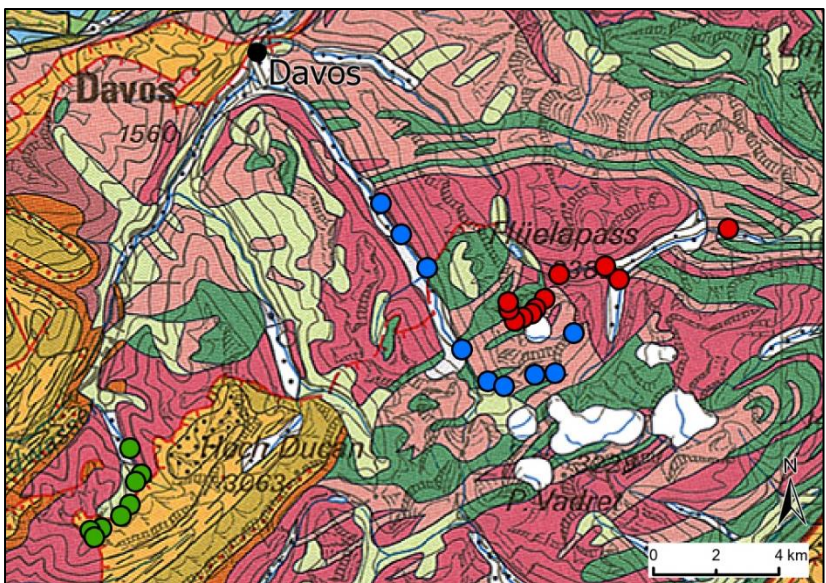
Figure 2: Close-ups of the study area, A: Aerial image, B: Physical map (base layer), C: Geological map (Geologie 500) where dark yellow areas: Dolomite, green areas: Amphibolite, dark and light red areas: Gneiss & Metagranitoids, light yellow areas: Moraines, white areas: Debris (Swisstopo, 2024)

2.1 Geology & Geomorphology

From a geological point of view, the Silvretta nappe on which the study area is situated roughly spans from Tiefencastel (Switzerland) in the west to the Imst (Austria) in the east. It has a complex geological history which will be briefly explained in the next paragraph. It helps to explain the local geology and geomorphology that can be found in the region (Leupold et al., 1935, Maggetti & Flisch, 1993).

The origins of the Silvretta nappe date back to the Paleozoic period. At this time in its early geological history, the region was subject to several metamorphic events and magmatic intrusions which shaped the geological base substantially. Extreme pressure and temperatures lead to the formation of gneissic rocks during the Proterozoic and the Paleozoic era (Maggetti & Flisch, 1993). For example, such a mixture of ortho- and paragneiss can be found on along the elevational gradient from the Fuorcla Radönt down to the lowest sampling locations of the Dischmatal (Transect 3). During the Paleozoic era, amphibolitic rocks were formed which are now part of the peak of the Schwarzhorn (Transect 2) (Leupold et al., 1935, Maggetti & Flisch, 1993). During the Variscan deformation, uplift led to compression and formed extensive folds. Then, in Triassic-Jurassic times, the Silvretta nappe subsided which led to the accumulation of dolomites and breccia (Maggetti & Flisch, 1993). Those sedimentary rocks are what the Büelenhorn is made of today (Transect 2) (Leupold et al., 1935). Then, during the Paleogene era, the nappe was being transferred onto the Pennine foreland where it is still present now (Maggetti & Flisch, 1993).

During the Pleistocene and Holocene series in the quaternary era, glacial advances and retreats further changed the visual appearance of the region. The moraines of the latest glacial maxima can be found at around 1800 – 2200 m. However, several retreat stages of moraines which are at least partially erased and or covered with debris during the Holocene series are characteristic for today's appearance (Leupold et al., 1935).

2.2 Climate

The closest weather station lies in Davos (2'783'519 / 1'187'459) at an elevation of 1594 m. The mean annual air temperature is 4.2 °C and mean annual precipitation is 1085 mm (mean over the last 30 years, 1994 – 2023) (MeteoSwiss, 2024).

2.3   Transects

As described above, the research area can be divided into three transects which differ in both geology and geomorphology.

2.3.1   Transect 1: Inneralpen – Büelenhorn [IB]

The first transect is situated south of Davos, close to Davos Monstein. Here, along an elevational gradient, eight sites were chosen on calcareous parent material. In terms of geomorphology, breccia glacial till and slope waste are predominant. The lowest site is located at 1840 m at Inneralpen, and the highest one lies on the top of the Büelenhorn at 2800 m, while the arial distance between these two sites is about 3 km. Along the slope, the vegetation changes from cushion plants at the highest site to grassland on the five sites in the middle and finally to a shrub and a forest site at the bottom. Generally, the sites are exposed to the north or north-east. Only the lowest site is orientated towards the west. Slope inclination varies between five and 28 degrees.
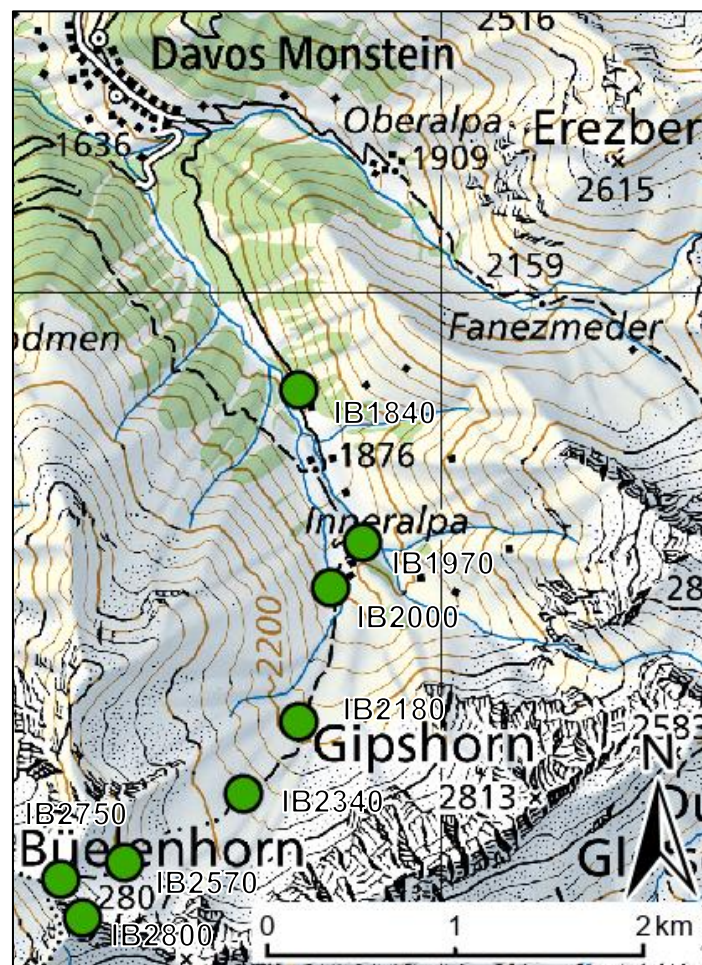
Figure 3: Close-up of the Inneralpen-Büelenhorn transect (Swisstopo, 2024)

Figure 4:Overview of the Inneralpen – Büelenhorn transect from the top of the Büelenhorn, IB2800 with cushion plants, IB2180 on grassland, and IB1970 with shrubs

2.3.2 Transect 2: Flüelapass – Schwarzhorn [FS]

The second transect is situated in the east of Davos. Along an elevational gradient, eleven sites were chosen on siliceous parent material. Here, the primary type of parent material is amphibolitic. However, the two sites at 2000 m and 2200 m also contain gneissic besides amphibolitic parent material. Blockfields, till and slope waste are the predominant geomorphological features in this transect. Eleven sites between 1830 m in the Val Susasca and the peak of the Schwarzhorn at 3100 m have been investigated. The aerial distance between these two sites is 7.4 km. At the peak we barley found any vegetation at all. A bit further down, we find one site with sparse vegetation, then two sites with cushion plants, and four sites are situated in grassland area. Out of the three bottom sites, two are shrubs sites and the lowest one is a forest site. The exposure of the individual sites varies considerably along this transect: While eastern and southern exposures tend to predominate at the top and towards the end of the transect, the middle sites are primarily orientated towards the north or north-east. Slope inclination is within four and 36 degrees.
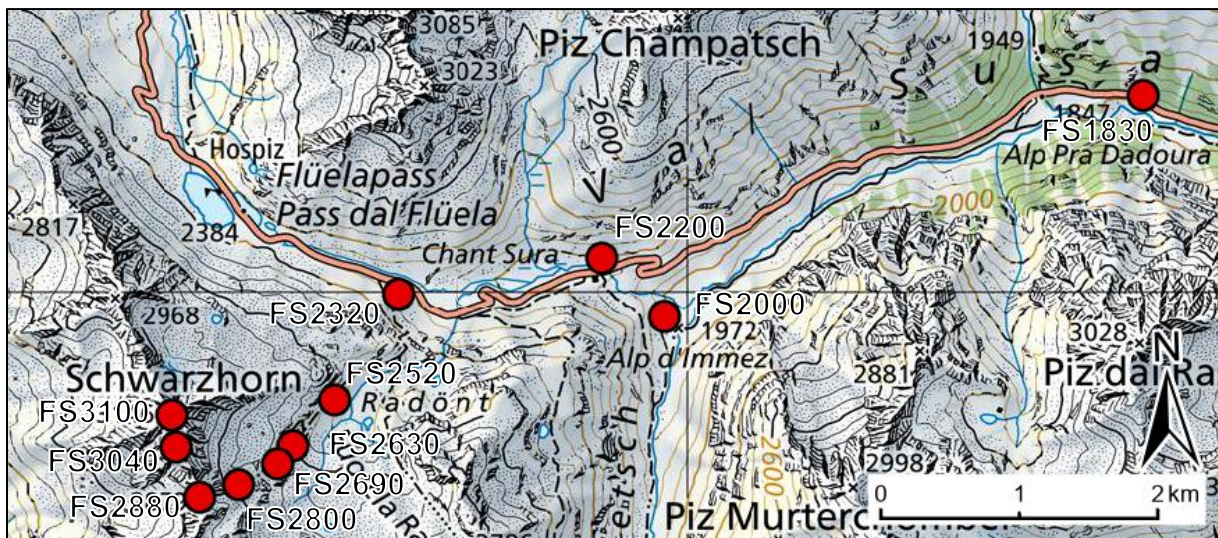
Figure 5: Close-up of the Flüelapass – Schwarzhorn transect

Overview of the FS transect from FS2690

FS3100

FS2320

FS2000

Figure 6: Overview of the Flüelapass – Schwarzhorn transect from the site FS2960, FS3100 with no vegetation, FS2320 on grassland, and FS2000 with shrubs

2.3.3   Transect 3: Dischmatal – Fuorcla Radönt [DR]

The third transect is situated in the Dischmatal, east of Davos. Nine sites have been chosen for this study on gneissic (silicate) parent material. Here, slope waste, till and solifluction are the primary geomorphological features. The lowest site is at 1750 m while the highest one is located at 2780 m close to the Fuorcla Radönt. These two sites are 7.3 km apart from one another. Cushion plants are the dominant form of vegetation at the highest site, then five grassland sites follow, and out of the lowest three sites, one is with shrubs and two are situated in a forest. In this transect, the four upper sites are characterized by a south-east to south exposure. At the sites further down in the Dischmatal, a westerly exposure dominates. Slope inclination varies between 15 and four degrees.
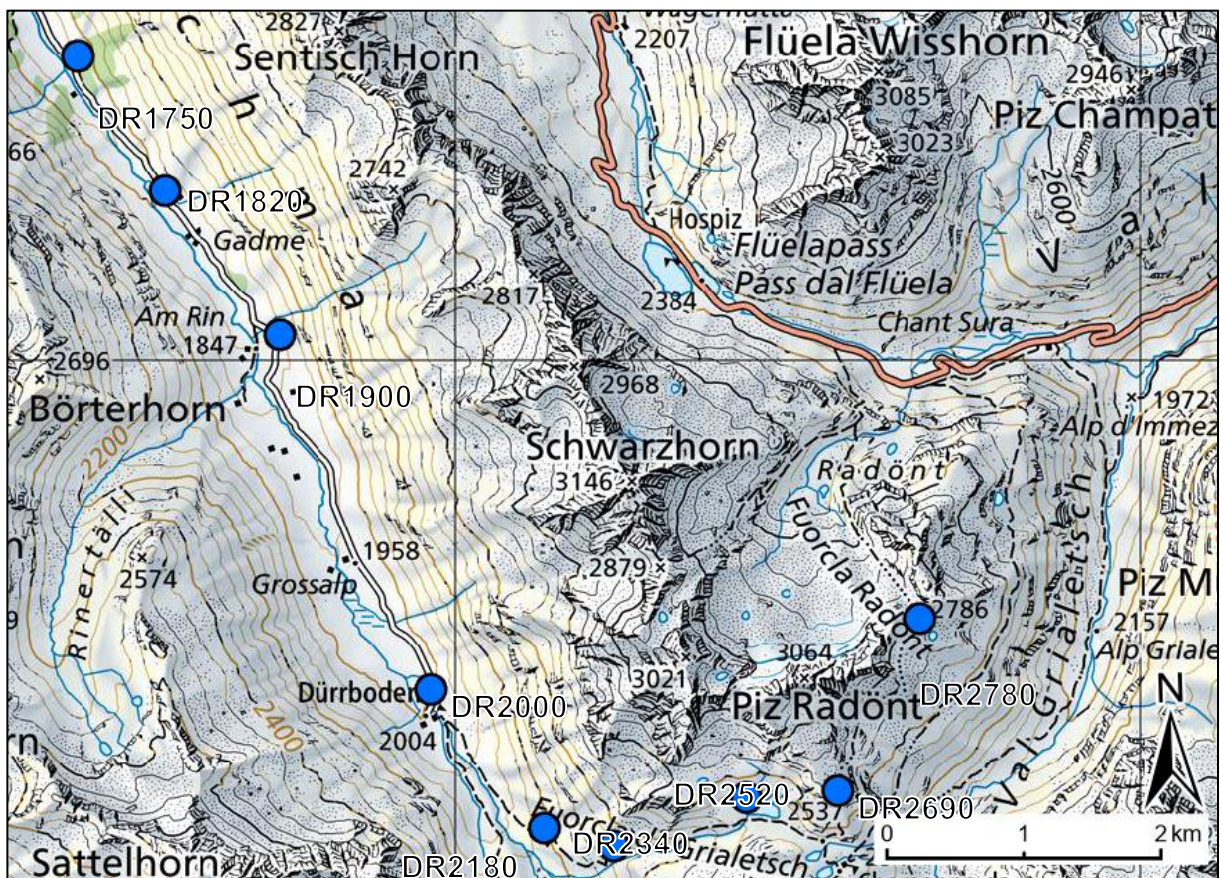
Figure 7:Close-up of the Dischmatal – Fuorcla Radönt transect (Swisstopo, 2024)

Figure 8: Overview of the Dischmatal – Fuorcla Radönt transect from the site DR2180, DR2780 with cushion plants, DR2340 on grassland, and DR 1750 in the forest

3 Methods

3.1 Field work

Field work was conducted during the vegetation period in 2023 while some data was already collected prior to the study as a part of the XThaw project (see 8.1.3). More precisely, a team of two or three people performed measurements and took samples once in mid-July, mid-August, and mid-September. To achieve the highest possible level of objectivity of implementation, one whole transect was completed each day. After reaching the highest point on foot, measurements and samples were taken at each site during the descent. That way, the team descended continuously along the elevation gradient, completing one site after the other. If it was not possible to walk an entire transect due to weather conditions or time constraints, the remaining sites were completed on the following day if possible, so that the temporal variability could be kept to a minimum. That way, each sampling-period lasted for three to four days, depending on the weather and personnel circumstances. In general, field work could be completed within the desired time span.

3.1.1 Sampling procedure

Plots have been sampled in the same way throughout the field season. To avoid a memory effect between the months, the measurement locations were slightly offset within the 5m radius, so measurements were taken on undisturbed soil in each repetition. This way, the local conditions at the site should be represented best. Each method will be explained in detail on the next pages.
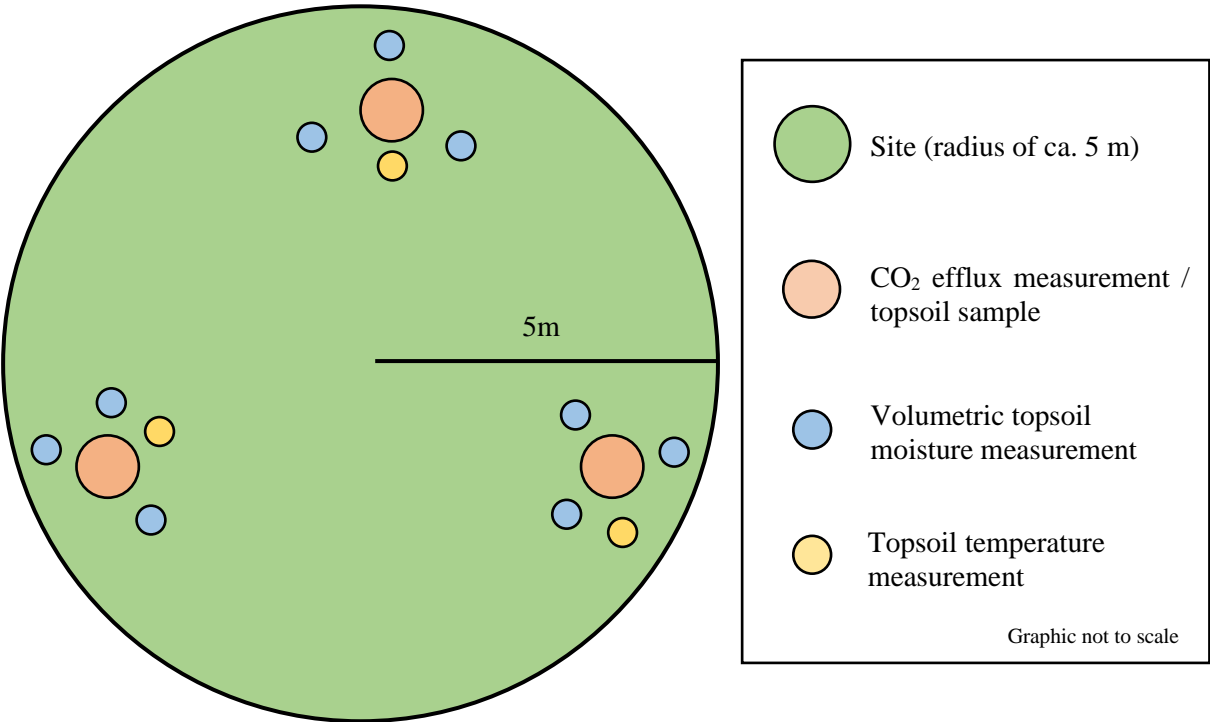
Figure 9: Conceptual representation of the sampling procedure in the field

3.1.2 Soil respiration

To determine soil respiration [SR], an airtight cylinder-like chamber was used. Inside the chamber, a CO_2-probe (*CO_2 Probe GMP343, Vaisala*) and an air temperature and humidity probe (*HMP75 probe, Vaisala*) are attached to the lid and connected to a handheld (*MI70, Vaisala*). This way, CO_2 emissions as well as relative humidity and air temperature could be measured at the same time. Additionally, a small fan connected to a battery was also fixed to the inside of the lid of the chamber which continuously mixed the air inside. The CO_2 measurements therefore included the CO_2 heterotrophic emissions from the soil, as well as the autotrophic CO_2 emission from the roots (Badraghi et al., 2021).

Along the elevational gradient, the air pressure settings in the handheld had to be adjusted to represent the environmental conditions. Thus, the air pressure was approximated in three steps to represent the local pressure conditions best: 750 hPa for the sites above 2500 m, 800 hPa between 2500 – 2000 m and 850 hPa for the measurements below 2000 m.

Before each measurement, the green vegetation cover was gently removed with a pair of scissors or picked out by hand to prevent the plants from conducting photosynthesis and thereby influencing the measurements. Here, care was taken not to rip out any roots or soil, which could have had an influence on the measurements. Next, the chamber was placed firmly onto the soil. Then, the height of the chamber was measured on four sides to better correct for any differences in the sampled volume that resulted from the chamber being dug into the soil for sealing.

Three measurements were taken at each site for each field work session. Each measurement lasted for 5 minutes, and a data point was taken every 5 seconds which resulted in 60 data points per efflux measurement. SR values from August of the gneissic transect (T3) were not considered for the analyses, as the measurements were several times higher than those in July and September. This could be due to incorrect application of the measurement devices or errors while calculating the data on that day. The measurement procedure had to be adapted for the high elevated sites of the calcareous (T1) and the amphibolitic transect (T2) (IB2800, FS3040 & FS3100) where a sealed-up cylinder would have been impossible to install due to the very rough and rocky terrain. Therefore, the cylinder was set on the ground and a tarp (3 m x 3 m) attached with tape to the chamber was used to collect the efflux from the soil. It was fixed to the ground at the edges with stones (see image below). Hereby, the measurement lasted for 15 minutes and measurements were taken every 15 seconds to achieve 60 data points to achieve a stable measurement series.

To calculate the CO_2 efflux, the CO_2 concentration in ppm were translated into µmol/l by including the assumed air pressure and measured air temperature. Then, the CO_2 efflux in $\mu mol\ m^{-2}\ h^{-1}$ and $mg\ m^{-2}\ h^{-1}$ were determined by including the volume of the cylinder and measurement time into the calculation.
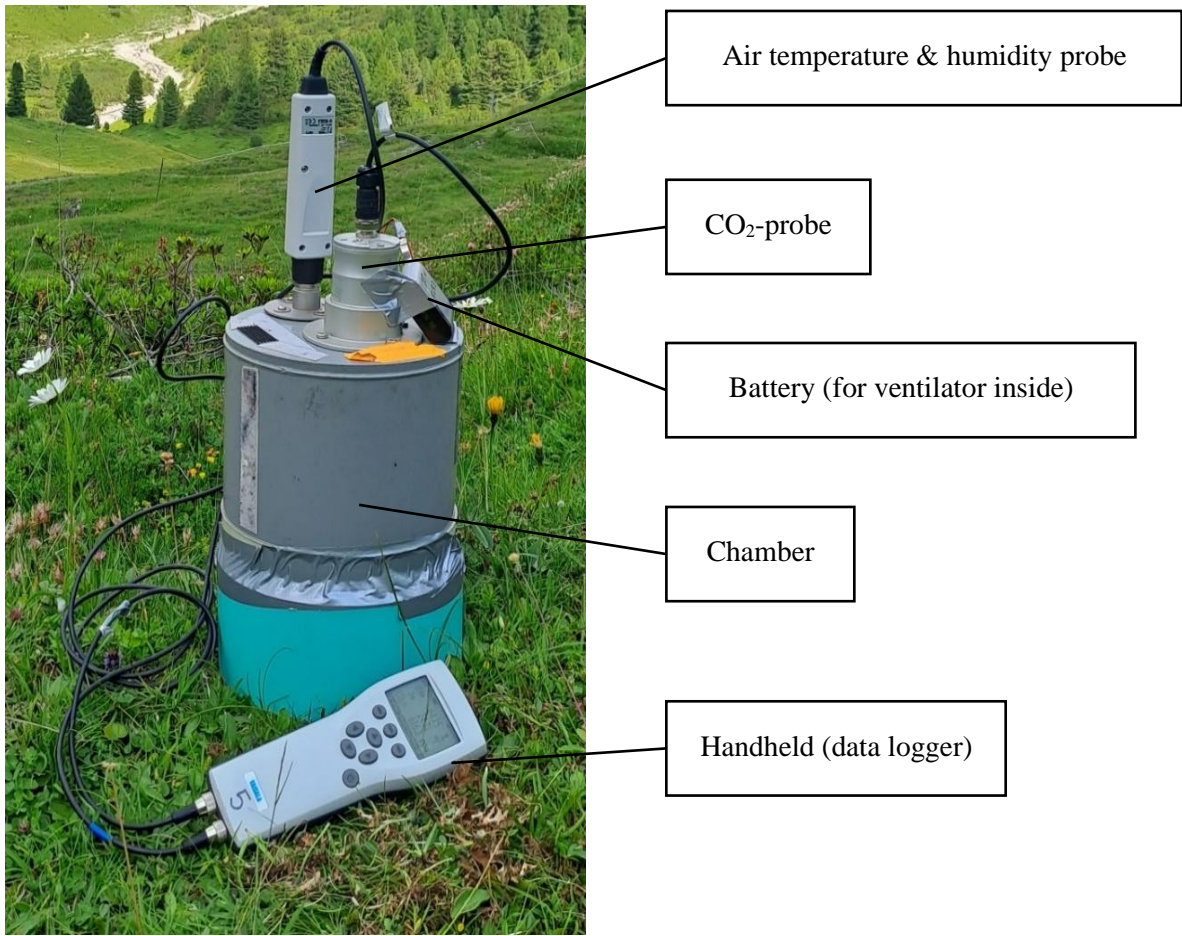
Figure 10: Soil respiration measurement cylinder on grass (upper picture) and cylinder with tarp on bare rocks (lower picture)

3.1.3 Topsoil temperature

The soil temperature was measured with a stick thermometer *(Checktemp, HANNA instruments*) at 5 cm depth. At each site, three temperature measurements were taken within a radius of 5 m to the center of the site. Generally, the aim was to have the best possible representation of soil temperature within the site area. Hence, the average temperature measurement per date and site was taken for a more solid soil temperature indication.

3.1.4 Volumetric soil moisture

The volumetric soil moisture was measured with a moisture probe (*ML3 ThetaProbe Soil Moisture Sensor*, *Delta-t Devices*) connected to a handheld (*HH2 Moisture Meter, Delta-t Devices*). This allowed the volumetric soil moisture to be determined directly in the field. The probe was inserted up to a depth of 5 cm into the soil. Unlike the soil temperature measurements, the volumetric soil moisture was measured nine times per site and date.
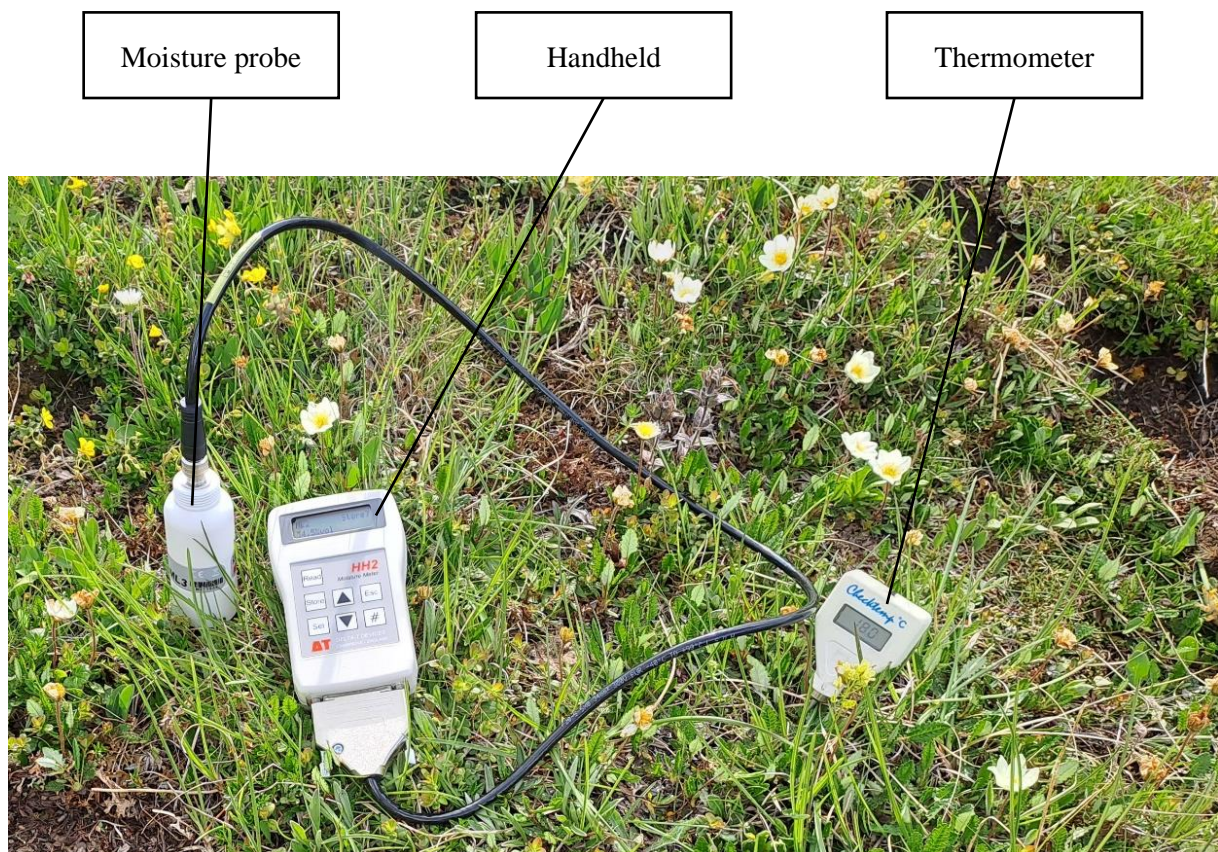
Figure 11: Moisture probe for volumetric soil moisture content measurements and thermometer for soil temperature measurements

3.1.5 Sample gathering

To determine the fine earth moisture, we excavated 5 cm of the topsoil where the CO_2-efflux measurements had been taken. We did not perform the efflux measurements / soil sampling at the same spot as a month before and shifted the measurement location slightly. Therefore, we also had a new soil sample every time which should represent the site best. Those samples were then wrapped in an airtight plastic bag to avoid any loss of moisture and labelled accordingly. Back at the WSL, the samples were stored at 5 °C in a refrigerator until they were further processed.

Plot after vegetation removal

Plot after excavation of topsoil

Figure 12: Plot after vegetation removal (upper picture) and after excavation of topsoil for the fine earth moisture (bottom picture)

3.2 Lab work

3.2.1 Fine earth moisture

The topsoil samples excavated in the field in summer 2023 were stored in airtight bags at WSL in a refrigerator. After the field work season, the bulk samples were weighed, and oven-dried at 105°C for 72h. Those samples were then weighed again and sieved (2 mm mesh size) to separate the fine earth from roots and stones. Later, fine earth moisture could be determined with the following formula where S_w = Bulk soil weight wet, S_d = Bulk soil weight dry, and L = Roots & Stones weight dry:

$$Water\ content\ fine\ earth\ [\%] = \frac{S_w - S_d}{S_w - L}$$

Fine earth (<2mm)   Roots and stones (>2mm)
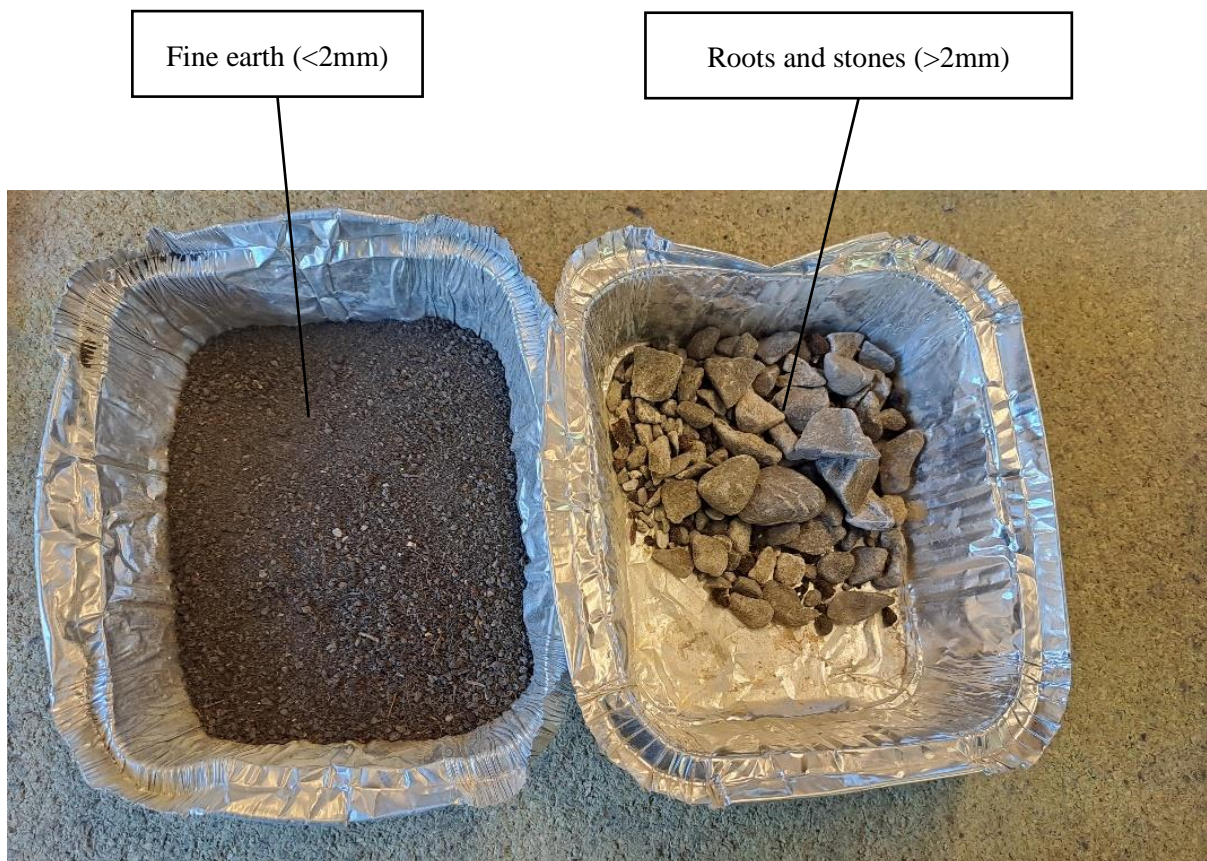
Figure 13: Sieved and oven-dried soil sample in aluminum trays separated into fine earth (left) and roots and stones (right)

3.2.2 Particle size fractionation

In this thesis, a physical particle size fractionation modified from Hagedorn et al., (2003), Amelung et al., (1999), and Guidi et al., (2023) has been conducted. The method is *"based on the premise that the association of soil particles and their spatial arrangement play a key role in SOM dynamics, because bioaccessibility is a prerequisite for decomposition"* (von Lützlow et al., 2007: p. 2184). The goal was to end up with four particle size fractions which correspond to the organic matter fractions:

Fraction	Corresponding organic matter	Particle size
Coarse sand fraction	*Coarse particulate organic matter [cPOM]*	*250–2000 µm*
Fine sand fraction	*Fine particulate organic matter [fPOM]*	*50–250 µm*
Silt & clay fraction	*Mineral-associated organic matter [MAOM]*	*<50 µm*
Dissolved fraction	*Dissolved fraction / organic carbon [DOC]*	*<0.45 µm*

Soils samples which had been collected during the field season 2022 and stored in a freezer at -20 °C were used to perform the particle size fractionation. In general, soil samples from a depth of 0 – 10 cm were used for the analysis. However, as the two sites FS3040 and FS3100 did not have any fine earth until 20 cm of depth, the samples were taken from a depth of 20 – 40 cm below the surface which represents the first layer of soil at those sites.

The total moisture of each sample was used to predict the dry-soil-weight. For this, an additional 5 g of moist soil (of the corresponding depth) was dried at 105°C for 72h. This was crucial for the first step to achieve the desired dry-soil:water ratio in the first step of the analysis.

3.2.2.1 Dissolved fraction ~ DOC

First, miliQ-water was added to the soil sample to get a dry-soil:water ratio of 1:6. This suspension was mixed with a magnet stirrer for an hour and placed into a falcon tube for centrifugation. Then, 30 ml of the suspension was removed from the falcon tube with a pipette and filtered using a syringe with a 45 µm cellulose acetate membrane filter. Later, the suspension was diluted 1:10 with miliQ water for total organic carbon analysis (*TOC-L, combined with an TNM-L and ASI-L, Shimadzu*).

3.2.2.2 Coarse sand fraction ~ coarse particulate organic matter [cPOM]

The soil remaining at the bottom of the falcon tube was added back to the beaker to achieve a dry-soil:water ratio of 1:5 (30 g of dry-soil: 150g of miliQ water). Then, the soils were ultrasonically dispersed in two steps to minimize the redistribution of SOM and the disruption of organic matter. Macroaggregates were dispersed ultrasonically at 60 J mL-1 with a probe-type sonicator (*Sonopuls HD 3200 homogeniser, Bandelin)* with 100W as output power. Next, the dispersed samples were carefully wet sieved to 250 µm and the suspension with the <250 µm fraction was placed into a glass beaker to sediment, while the coarse sand fraction (250 – 2000 µm) on the sieve was transferred to an aluminum pan and dried in a drying oven at 40 °C. When completely dry, the coarse sand fraction was weighed.

3.2.2.3 Fine sand fraction ~ fine particulate organic matter [fPOM]

Together with the weight of the coarse sand fraction (250 – 2000 µm), the amount of water that had to be removed from the <250 µm suspension could be calculated. This is important since a lower soil:water ratio (here 1:10) shortened the sonification time in a further step. Here, excess water from the <250 µm fraction suspension was removed with a pipette, placed in falcon tubes, and centrifuged. The water in the falcon tubes was then removed with a pipette, and the remaining soil was returned into the <250 µm suspension. Thus, a dry-soil:water ratio of 1:10 was achieved.

Later, the suspension was redispersed at 440 J/mL $^{-1}$ (total of 54912 J) at 100 W. To prevent overheating, the beaker was placed in an ice bath due to the long sonification time. The dispersed samples were then wet sieved to 50 µm. The fraction which stayed on the sieve was transferred into an aluminum pan and dried at 40 °C before weighing when completely dry.

3.2.2.4 Silt & clay fraction ~ Mineral-associated organic matter [MAOM]

The suspension in the sieve tray was also transferred into an aluminum pan and then dried at 40 °C. When completely dry, the weight of the (<50 µm) fraction could be determined as well.

3.2.2.5 Mass recovery

Each fraction was weighed in the end and the weight ratios could be determined. However, during the entire process, some of the material got lost. On average, the mass recovery was 94% (SE = 2.7%). This is comparable with Guidi et al. (2023) who achieved a mass recovery of 96.3% (SE = 0.4%) from which the method was modified.
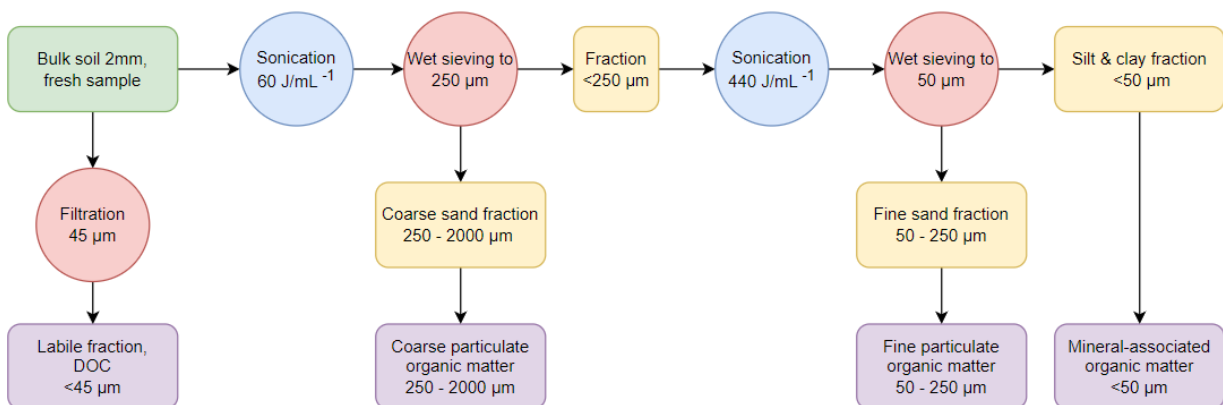
Figure 14: Schematic representation of the physical soil fractionation procedure
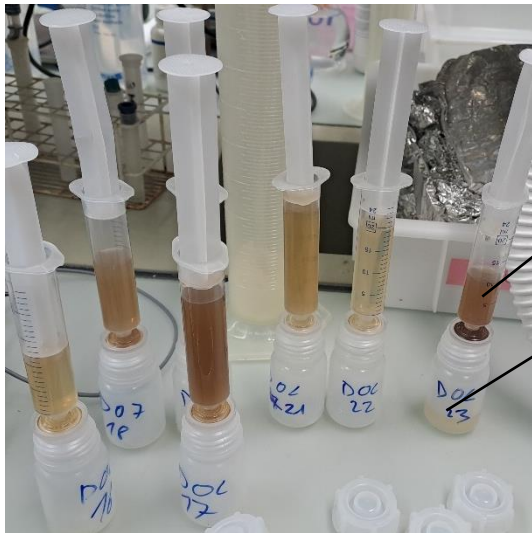
Syrinye with cellulose filter (45 µm)

Dissolved fraction (<45 µm)

Coarse sand fraction (<250 – 2000 µm)

Sieve (mesh size: 250 µm)

Fractions (<250 µm)
with excess water

Fine sand fraction (250 – 50 µm)

Sieve (mesh size: 50 µm)

Silt & clay fraction (<50 µm)
with excess water

Figure 15: Four different fractions which have been separated from each other during the physical soil fractionation

3.2.3 Element analysis & Isotope ratio mass spectrometry

The three solid fractions (coarse sand fraction (250 – 2000 µm), fine sand fraction (50 – 250 µm), silt & clay fraction (50 – 0.45 µm)) were milled to fine powder for further analysis with a ball mill (*Mixer mill MM 400, Retsch*).

Later, the milled samples were weighed and packed in tin cups. The central lab at WSL analyzed the samples for C and nitrogen [N] stocks as well as for $\delta^{13}C$, and $\delta^{15}N$ values by combustion in an elemental analyzer (*Euro EA3000, Euro Vector*) combined with an isotope ratio mass spectrometer (*Delta V Advanced, Thermo Scientific*).

3.3 Data analysis

In general, data collection and aggregation were carried out using Microsoft Excel. Then, R Studio has been used to further process the data, conduct statistical tests, and create plots.

3.3.1 Calculations of soil organic carbon & C/N concentration

Together with the weight ratios of the particle size fractionation, the C pools as well as C/N ratios could be determined for each fraction with the results from the elemental analyzer. Due to the limited time horizon of this master's thesis, the soil samples from the calcareous transect (T1) could not be fumigated to assess their real SOC stock. Therefore, values of SOC for each fraction were approximated by using the isotope ratio $\delta^{13}C/\delta^{12}C$ in the bulk soil sample as follows:

$$\frac{Bulk \; \frac{\delta^{13}C}{\delta^{12}C}}{Bulk \; SOC} = \frac{\frac{\delta^{13}C}{\delta^{12}C} \; in \; fraction}{SOC \; in \; fraction}$$

The elemental analyzer was unable to determine all C and N values due to excessively high or low initial sample weights. Therefore, the total SOC stocks which have been previously assessed in the frame of the XThaw project were used to determine some of the missing values. Unfortunately, not all values could be calculated as necessary data was sometimes missing which led to slightly incomplete data columns. Then, the SOC concentration within each fraction [%C], the contribution of the fraction to the total SOC [%], the SOC stock in the fraction [kg m^{-2}], and the C/N ratio were calculated.

In the end, SOM in the coarse sand and fine sand fraction has been allocated to the labile coarse and fine POM fraction [cPOM and fPOM respectively]. Carbon in these fractions was labeled particulate organic carbon [cPOC and fPOC respectively]. Soil organic matter in the silt & clay fraction was assigned to the stable MAOM fraction and C in that fraction was labelled mineral-associated organic carbon [MAOC] (Guidi et al., 2023). Within the dissolved fractions, SOC in g C m^{-2} has been calculated by using the corresponding soil density and depth (0 – 10 cm).

3.3.2 Temperature sensitivity Q_{10}

The temperature sensitivity [Q_{10}] values were not calculated separately for each site as the amount of temperature and corresponding SR data was relatively small and led to inconsistent results. Therefore, a Q_{10} of 3 was selected for all sites according to Hagedorn et al. (2010c) who found this value suitable for SR at Stillberg (2180 m) in the Dischmatal close to Davos which is within in the same area as the present study. The Q_{10} of 3 was then used to model a standardized SR at 10° [SR_{10}] for each site according to the following formula where SR_{10} is the soil respiration at 10°C, SR is soil respiration, Q_{10} is the temperature sensitivity of 3, and soil temperature is ST:

$$SR_{10} = SR * Q_{10}^{\frac{10-ST}{10}}$$

3.3.3 Statistical analysis

Linear mixed effect models were used to assess the effect of elevation, transects, and the monthly variations (fixed effects) on response variables. The transect integrates parent material and topographic variables while elevation integrates temperature and vegetation. Elevation can be used as a proxy for temperature as it is ultimately linked to it. Similarly, vegetation changes along elevational gradients with elevation (Egli & Poulenard, 2016). Moreover, location (site) was used as a random effect in the model according to the experimental design of this study.

The model has been applied for the entire transects while including all available data. However, SR data from the gneissic transect (T3) in August was excluded due to unreasonably high values compared to the other two months and transects. Moreover, it was found that irregularities in soil parameters occurred most in the locations with shrubs and forest. Therefore, the same model has also been applied for the shortened transects resp. a subset of the transect above the treeline while excluding sites with shrubs and forest.

Additionally, the parameter transect (T1, T2 & T3) was replaced with parent material (calcareous or siliceous, named *Bedrock* in the model / code) in a second model to better understand the influence of the parent material on the response variables.

For the fractions, a different model was used. Here, elevation, transect, and fraction were used as fixed effects and location as a random effect. As for the first model, transect was replaced with the parent material type (calcareous or siliceous). The Type 3 sum of squares ANOVA was used to determine p and F values for each model with a significance level of *p < 0.05*. To assess the normality of residuals, a Shapiro-Wilk normality tests was conducted. However, not all residuals were normally distributed. Therefore, a (log + 0.1) transformation was considered to meet the models' requirements for normally distributed residuals (as for example performed in Fetzer et al., 2024). However, this step rarely led to normally distributed residuals which is why it was then decided not to transform the data in order to treat the data set uniformly. Columns with non-normally distributed residuals data were marked with *.

4 Results

4.1 Site conditions

4.1.1 Soil parameters
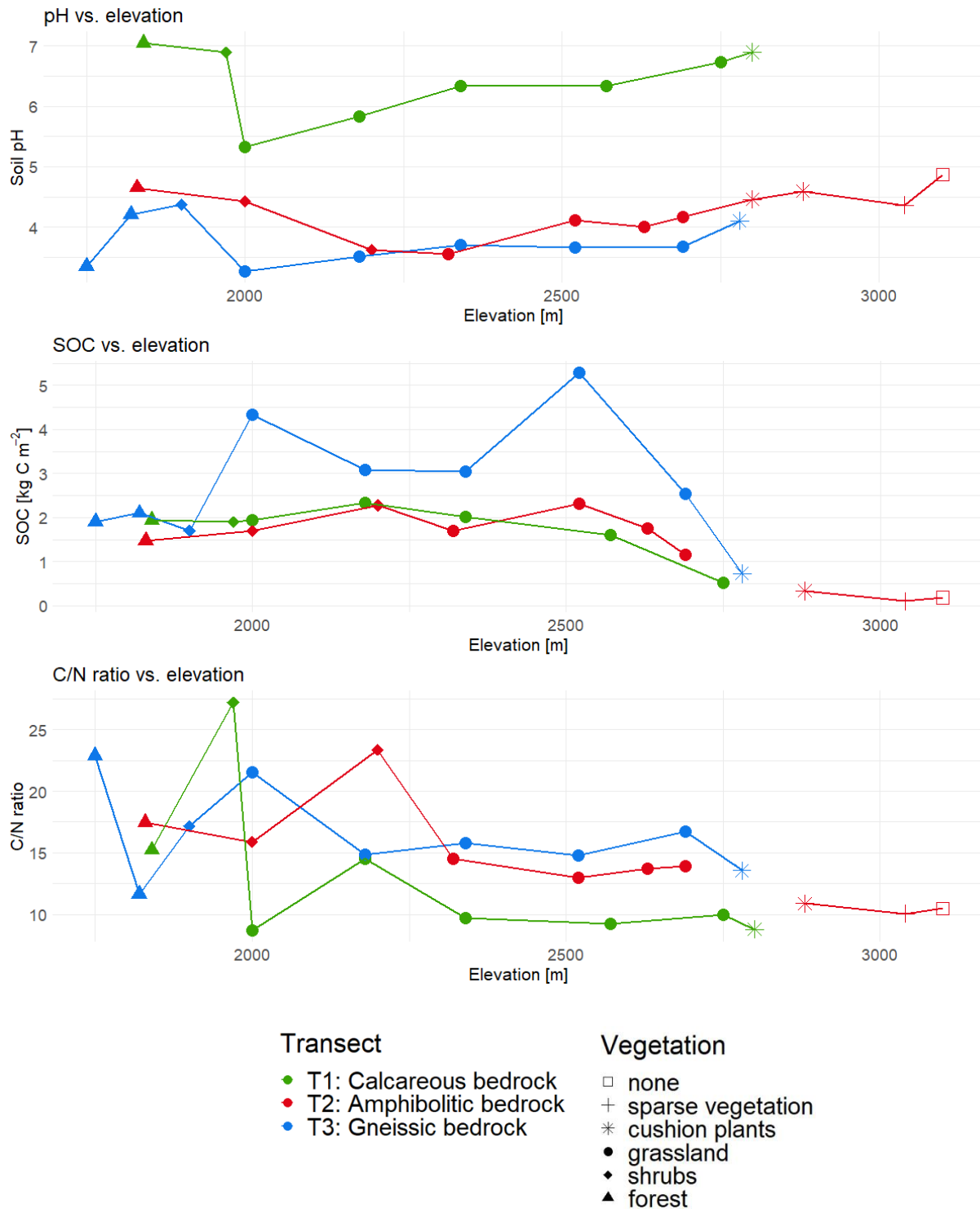
Figure 16: Topsoil (0 – 10 cm) parameters (pH, SOC, CN) which were collected in preliminary stages of the thesis as part of the XThaw project

Overall, soil pH at 0 – 10 cm depth gradually decreases from the sites with little or no vegetation towards the grassland sites. Then, soil pH increases on all parent materials in the shrub and forest sites in lower elevations. There was no significant pattern in soil pH with elevation across the entire elevational gradients ($p_{Elevation}$ = 0.9). However, for the sites above the treeline, pH decreases with decreasing elevation ($p_{Elevation}$ = <0.01).

The sites on calcareous parent material show pH values in the topsoil between 5.3 and 7, whereas the two other transects are generally more acidic: Values range between 3.5 and 4.9 for the amphibolitic sites and between 3.3 and 4.4 for the sites on gneissic parent material. The model did not reveal any statistical significances in soil pH between the transects ($p_{Transect}$ = 0.22 for all sites resp. 0.13 for the sites above the treeline). Surprisingly, the second model which has been conducted with the two parent materials instead of the three transects did not provide any significant differences either although the calcareous topsoils show much higher pH values.

Soil organic carbon [SOC] stocks at 0 – 10 cm depth increase along all three transects from the high elevated sites towards the grassland sites before they then decrease towards the sites with shrubs and forest. The general increase in SOC with decreasing elevation is significant for the entire transect as well as for the sites above the treeline ($p_{Elevation}$ = <0.01 resp. <0.01). Highest values of SOC stocks are reached in all transects in grassland sites (IB2180: 2.3 kg C m^{-2}, FS2520: 2.3 kg C m^{-2}, and DR2520: 5.3 kg C m^{-2}) while lowest values close to zero can be found at the highest nival sites. Although the gneissic topsoils contain on average 1.8 times more SOC than the other two transects, differences among the three parent materials are neither statistically relevant for the entire transects nor for the sites above the treeline. This also applies to the second model (with parent material instead of transects). However, the $p_{Elevation * Transect}$ = 0.04 suggests that elevational patterns between the three parent materials are different.

The C/N ratio at 0 – 10 cm depth increase gently throughout the entire elevational gradient with decreasing elevation ($p_{Elevation}$ = <0.01) although there is no systematic pattern for the lower sites. The sites above the treeline do not show a distinct pattern with elevation ($p_{Elevation}$ = 0.72).

In the upper half of the transect, the calcareous transect generally shows smaller C/N ratios than the siliceous ones. This pattern is no longer continued at lower elevated sites.

The three transects neither differ significantly in C/N ratio along the entire length of the transects nor along the sites above the treeline. However, when using parent material instead of transect in the model, the C/N ratios are significantly higher on siliceous than on calcareous parent material ($p_{Bedrock}$ = <0.01 for all sites and $p_{Bedrock}$ = <0.01 for the sites above the treeline). Also, the elevational pattern differs between the parent material types in the parent material model ($p_{Elevation * Bedrock}$ = <0.01 for all sites and $p_{Elevation * Bedrock}$ = <0.01 for the sites above the treeline).

4.1.2 Field measurements
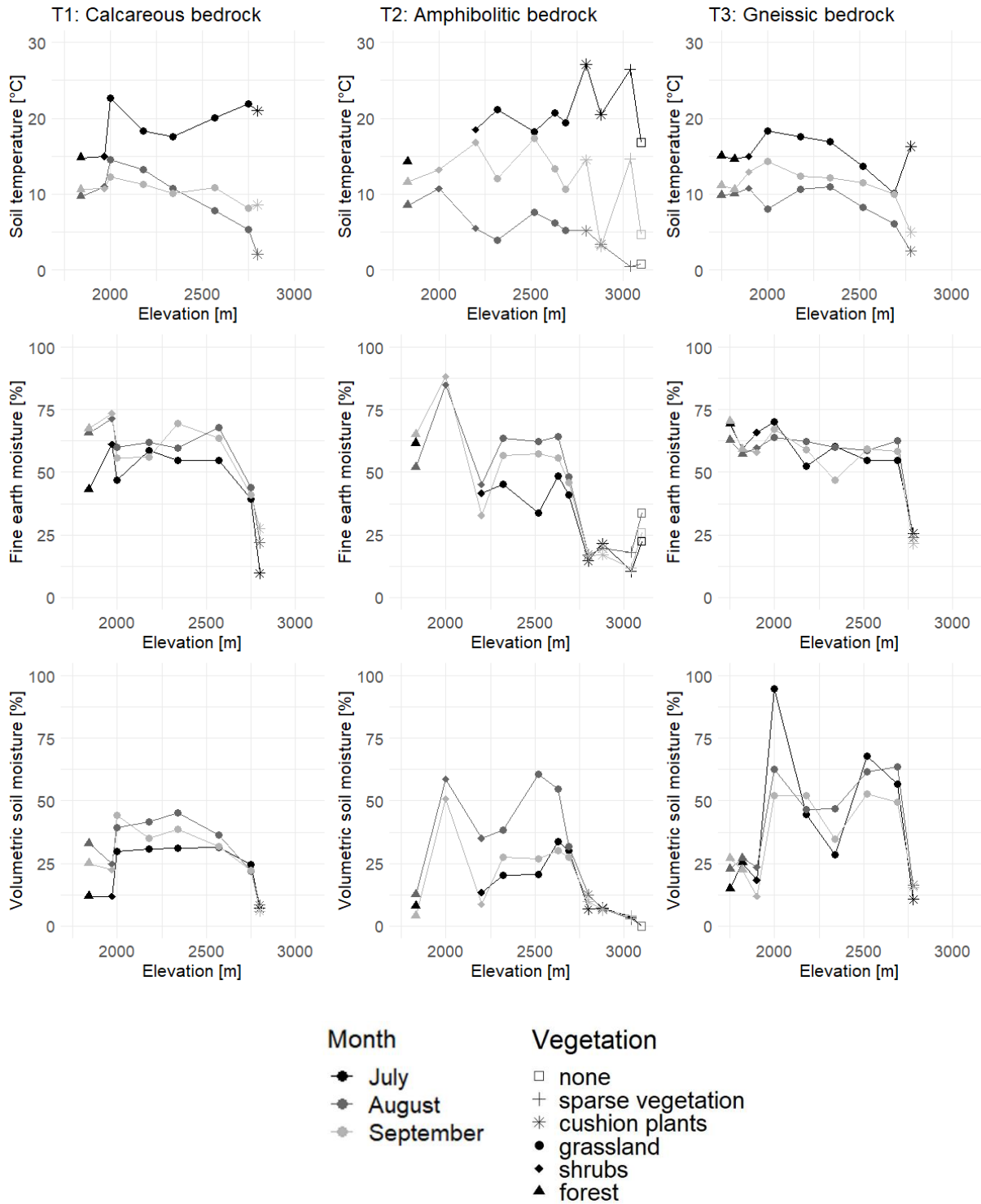
Figure 17: Field measurements in the topsoil (0 – 5 cm) measured in July, September, and August 2023. Data shows means of three replicas at each site and time

Soil temperatures measured throughout the measurement campaign vary with elevation on each transect. Overall, they increase with decreasing elevation ($p_{Elevation} = 0.02$). The same applies to the sites above the treeline ($p_{Elevation} = < 0.01$). Across the three parent materials, there are no relevant differences in soil temperature across the entire dataset as well as for the subset ($p_{Transect} = 0.84$ for both transect lengths). Soil temperatures in July are highest for each parent material with an average temperature of 18.2 °C. In August, they are lowest with a mean of 7.5 °C while mean soil temperatures in September are 11.2 °C. Thus, the monthly variations as well as the interaction between elevation and monthly variations are highly relevant for the entire transects ($p_{Month} = 0.01$, $p_{Elevation * Month} = < 0.01$). Only the interaction between monthly variations and elevations are relevant for the sites above the treeline ($p_{Elevation * Month} = 0.03$).

Overall, fine earth moisture rises with decreasing elevation. Especially the sudden increase from sparse vegetation to grassland sites is strongly pronounced. For all parent material types and throughout the measurement period, fine earth moisture increases with decreasing elevation for both the entire as well as for the sites above the treeline ($p_{Elevation} = <0.01$ resp. <0.01). However, there are no statistical differences between the three transects ($p_{Transect} = 0.49$) nor are there any systematic patterns between the three months ($p_{Month} = 0.45$) or any interaction when looking at the entire transects. The same applies to the shortened transects ($p_{Transect} = 0.49$ resp. $p_{Month} = 0.45$).

Across the whole dataset, volumetric soil moisture does not follow any organized pattern along the elevational gradients ($p_{Elevation} = 0.51$). However, the sites above the treeline show a significant elevational pattern ($p_{Elevation} = <0.01$). There are no relevant differences between the three parent materials ($p_{Transect} = 0.48$) nor are there any significant differences between the months ($p_{Month} = 0.15$) across the entire length of the transects. Still, the interaction of the transect and the month as well as the combination of all three fixed effects reveal significant differences ($p_{Transect * Month} = 0.01$ resp. $p_{Elevation * Transect * Month} = 0.02$).

4.2 Soil respiration
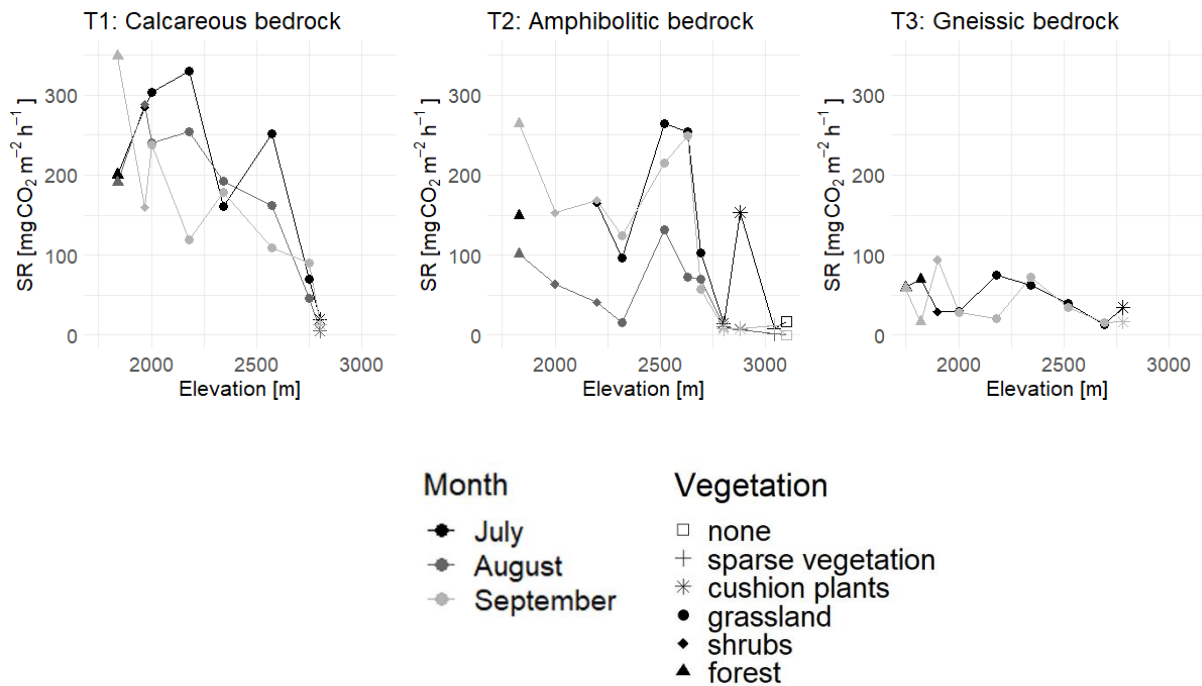
Figure 18: SR rates measured in July, September, and August 2023. Data shows means of three replicas at each site and time

Soil respiration [SR] shows a diverse pattern over all months and transects. Still, there is an overall rise in SR rates with decreasing elevation along the elevational gradients which is highly significant for both transect lengths ($p_{Elevation} = <0.01$ for both sections: entire gradient and above treeline).

Calcareous parent material has the highest mean SR rates with 177 mg CO_2 m^{-2} h^{-1} followed by amphibolitic parent material with 93 mg CO_2 m^{-2} h^{-1} and gneissic parent material with 42 mg CO_2 m^{-2} h^{-1}. Soil respiration on calcareous parent material is therefore more than twice as high than on siliceous parent material. This is reflected by the statistical analysis where both models for the respective transect sections show significant differences between the parent materials ($p_{Transect} = <0.01$ for the entire transect and $p_{Transect} = 0.02$ for the sites above the treeline).

In the second model (with parent material instead of transects), SR on siliceous parent material was significantly smaller than on calcareous parent material ($p_{Bedrock} = <0.01$ for the entire transect and $p_{Bedrock} = 0.01$ for the sites above the treeline).

The elevational pattern is significantly different between the three entire transects ($p_{Elevation} = 0.01$) but not for the sites above the tree line. No significant differences exist between the three measurement dates ($p_{Month} = 0.36$ for the entire transect and $p_{Transect} = 0.23$ for the sites above the treeline).

30
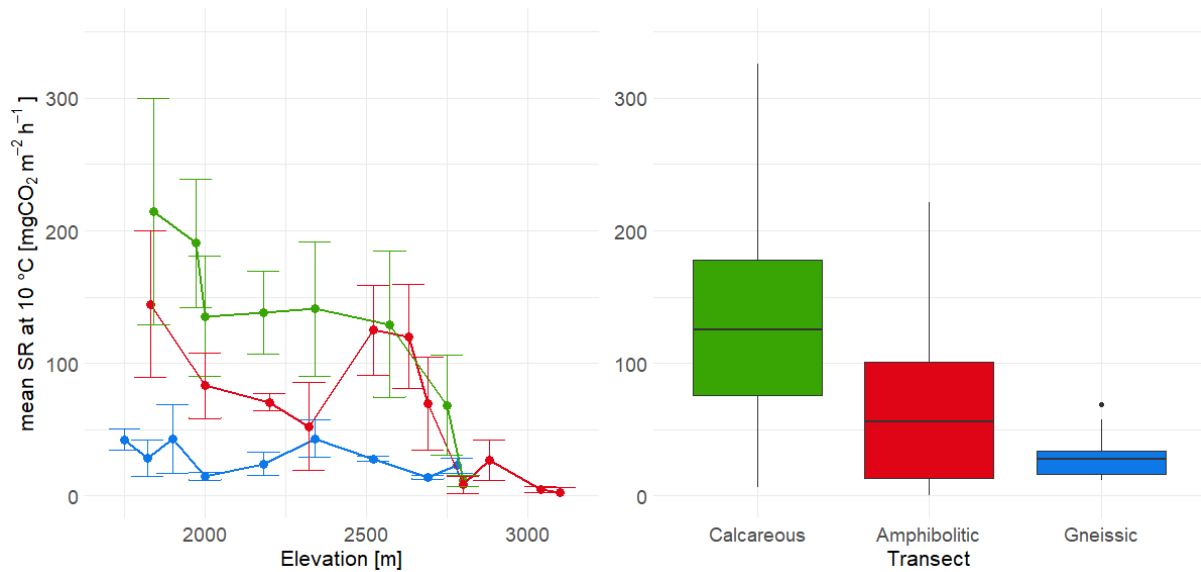
Figure 19: Standardized SR$_{10}$ across the three parent materials and months with standard error bars

The standardized soil respiration at 10°C [SR$_{10}$] also increases with decreasing elevation across entire transects (p $_{Elevation}$ = <0.01) as well as for the sites above the treeline (p $_{Elevation}$ = 0.01). The median SR$_{10}$ is highest on calcareous parent material (125 mg CO$_2$ m^{-2} h^{-1}), whereas amphibolitic (55 mg CO$_2$ m^{-2} h^{-1}), and gneissic parent material (27 mg CO$_2$ m^{-2} h^{-1}) show lower values. Hence, there is a significant impact of the parent material across entire transects (p $_{Transect}$ = <0.01). No such impact exists for the shortened transects (p $_{Transect}$ = 0.08). The elevational pattern differs between the three types of parent material which is only significant for the entire transects (p $_{Elevation * Transect}$ = 0.01).

The second model (with parent material instead of transects) provided a similar output where calcareous sites show significantly higher SR$_{10}$ values across all sites but not for the sites above the treeline.

Table 1: Results of the linear mixed effects model testing the statistical significance of elevation, **transect**, and monthly variations on response variables. Bold values are p < 0.05. Note that not all residuals are normally distributed. Collums marked with * indicate a non-normal distribution of the residuals

All sites

Statistic	Exposition* F	Exposition* p	Slope* F	Slope* p	pH F	pH p	SOC* F	SOC* p	C/N* F	C/N* p	ST F	ST p	Fine earth moisture* F	Fine earth moisture* p	Volumetric soil moisture* F	Volumetric soil moisture* p	SR F	SR p	SR$_{10}$* F	SR$_{10}$* p
Elevation	12.02	**<0.01**	9.29	0.96	2.25	0.90	7.78	**<0.01**	37.53	**<0.01**	5.86	**0.02**	23.85	**<0.01**	0.46	0.51	28.00	**<0.01**	27.05	**<0.01**
Transect	2.53	0.09	1.35	0.43	3.53	0.22	1.47	0.23	1.29	0.44	0.18	0.84	0.73	0.49	0.76	0.48	9.57	**<0.01**	8.90	**<0.01**
Month											4.63	**0.01**	0.82	0.45	1.97	0.15	1.48	0.24		
Elevation*Transect	0.85	0.43	0.93	0.52	0.69	0.59	3.33	**0.04**	2.06	0.33	0.40	0.67	0.88	0.43	1.26	0.30	5.54	**0.01**	5.10	**0.01**
Elevation*Month											15.43	**<0.01**	0.80	0.46	1.02	0.37	0.99	0.38		
Transect*Month											1.65	0.18	1.01	0.41	1.57	0.20	1.30	0.29		
Elevation*Transect*Month											1.91	0.13	0.67	0.61	1.09	0.37	0.83	0.48		

Sites above treeline

Statistic	Exposition* F	Exposition* p	Slope* F	Slope* p	pH F	pH p	SOC* F	SOC* p	C/N* F	C/N* p	ST F	ST p	Fine earth moisture F	Fine earth moisture p	Volumetric soil moisture F	Volumetric soil moisture p	SR F	SR p	SR$_{10}$* F	SR$_{10}$* p
Elevation	0.20	0.88	0.77	0.89	36.77	**<0.01**	38.31	**<0.01**	36.08	0.72	14.91	**<0.01**	16.66	**<0.01**	14.42	**<0.01**	17.42	**<0.01**	9.22	**0.01**
Transect	12.30	0.08	0.60	0.63	6.42	0.13	1.24	0.31	6.38	0.14	0.17	0.84	0.50	0.62	0.35	0.71	5.27	**0.02**	3.04	0.08
Month											0.80	0.46	1.38	0.27	1.27	0.30	1.57	0.23		
Elevation*Transect	7.45	0.12	0.32	0.76	14.62	0.06	0.51	0.61	2.81	0.26	0.38	0.69	0.54	0.59	0.32	0.73	3.63	0.05	2.06	0.16
Elevation*Month											3.98	**0.03**	0.52	0.60	0.66	0.52	0.94	0.40		
Transect*Month											1.44	0.25	1.79	0.16	4.02	**0.01**	2.14	0.12		
Elevation*Transect*Month											1.46	0.24	1.58	0.21	3.47	**0.02**	1.72	0.19		

4.3 Soil fractionation

4.3.1 Soil organic matter fractions
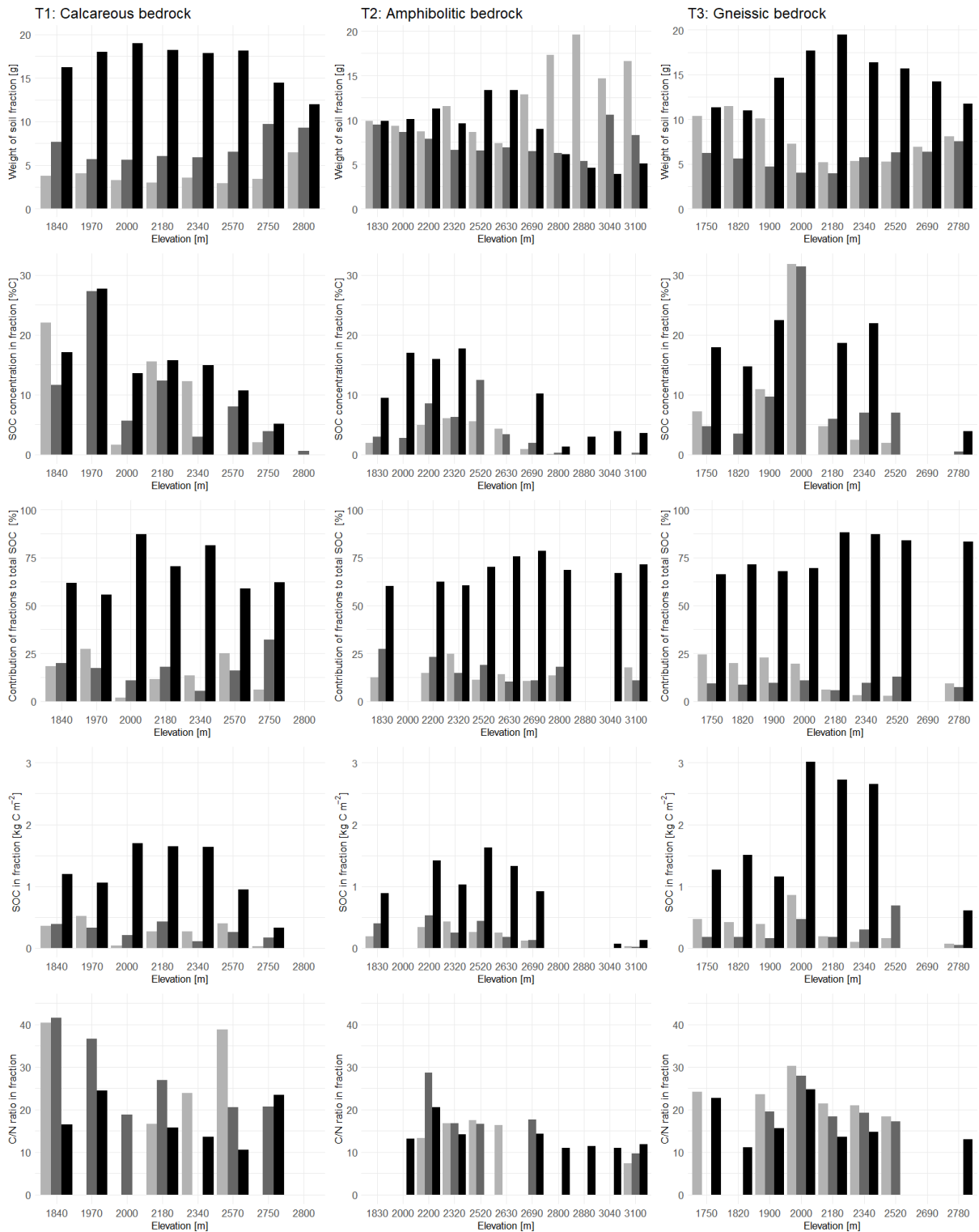
Figure 20: Weight of the soil fractions, SOC concentration within the fraction, proportion of bulk SOC in the fraction, SOC pool in the fraction, and C/N ratio in the fraction in the topsoil (0 – 10 cm resp. 20 – 40 cm for FS3040 & FS3100) across all three transects

In terms of fraction mass, none of the three fractions shows any statistically significant pattern with elevation. The effect of the parent material is only significant for the weight of the coarse particulate organic matter [cPOM] ($p_{Transect} = 0.05$) where we also find a relevant interaction of elevation and parent material ($p_{Elevation * Transect} = 0.03$). The parent material does not affect the weight of fine particulate organic matter [fPOM] and mineral-associated organic matter [MAOM].

Neither the elevation nor the parent material or any interaction has a statistically significant effect on the SOC concentration within each fraction. The same applies to the contribution of fractions to total SOC. Elevation is only statistically relevant on the SOC stock in the cPOM ($p_{Elevation} = 0.02$) whereas the SOC stock within the fPOM and MAOM are not significantly affected by elevation. The SOC stocks within the fractions do not show any significant effect of the parent material.

Although they do not show a linear pattern with elevation, the mass of MAOM and the contribution of mineral-associated organic carbon [MAOC] to the total SOC are generally greatest at elevations between 2000 m and 2700 m which are covered in grasslands.

The C/N ratio in the fPOM fraction ($p_{Elevation} = <0.01$) increases significantly with decreasing elevation while the effect of elevation is not significant for the cPOM ($p_{Elevation} = 0.65$) and MAOM ($p_{Elevation} = 0.88$). There is no statistical valid influence of the transect on the C/N ration in any of these three fractions. Moreover, the parent material model does not show any significant p values for any of the response variables.

4.3.2   Fractions' model

The fractions' model has been used to assess whether the response variables within the fractions (mass, SOC concentration, contribution of fractions to total SOC, SOC stock, and C/N ratio) differ between elevation, transect, and fraction. The fractions' mass ($p_{Elevation} = <0.01$) as well as the fractions' C/N ratio ($p_{Elevation} = <0.01$) are highly elevation dependent. The type of parent material is not significant in any of the fractions' parameters. Furthermore, fractions' mass ($p_{Fraction} = <0.01$), SOC concentration ($p_{Fraction} = 0.01$), and C/N ratio ($p_{Fraction} = 0.02$) differ between the fractions.

For the fraction's mass and the proportion of bulk SOC, interactions of elevation & fraction, transect & fraction, and elevation, transect & fraction are significant. The SOC stock in the fractions is not significantly influenced by any of the fixed effects. As for the other models, the transect has also been replaced with parent material to see whether there are differences between calcareous and siliceous sites. However, it did not show any significant p values for any of the response variables.

4.3.3 Dissolved fraction
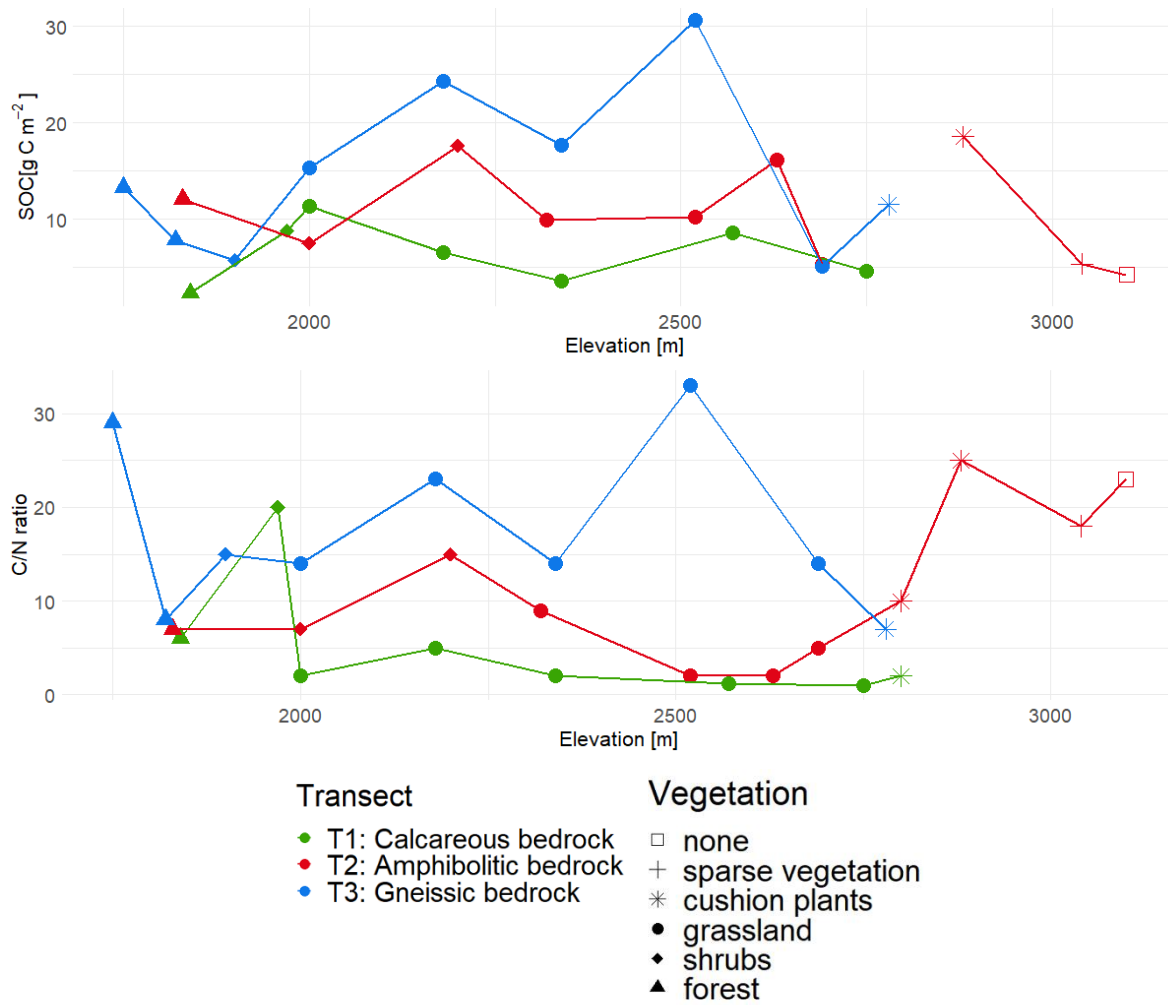
Figure 21: SOC stocks and C/N ratio in the dissolved fraction in the topsoil (0 – 10 cm)

There is no obvious pattern visible in SOC stocks fraction as well as in the C/N ratio along the gradients within the dissolved. Nevertheless, there is a statistically significant decrease in SOC stock of the dissolved fraction ($p_{Elevation}$ = 0.03) as well as C/N ratio ($p_{Elevation}$ = <0.01) with decreasing elevation. Neither the first model with the three transects nor the second one with the two parent materials found any significant p values for SOC stocks or C/N ratio in the dissolved fraction.

*Table 2: Results of the linear mixed effects model testing the statistical significance of elevation and transect on response variables within the soil fractions for the entire transect length. Bold values are p < 0.05. Note that not all residuals are normally distributed. Collums marked with * indicate a non-normal distribution of the residuals. The third table row shows the results of the soil fractionation model where the effects of elevation, transect and fraction on response variables have been investigated*

	Coarse sand fraction / cPOM										Fine sand fraction / fPOM									
	Mass*		SOC concentration *		Contribution of cPOM to total SOC *		SOC stock*		C/N ratio*		Mass*		SOC concentration *		Contribution of fPOM to total SOC *		SOC stock		C/N ratio*	
Statistic	F	p	F	p	F	p	F	p	F	p	F	p	F	p	F	p	F	p	F	p
Elevation	5.05	0.99	11.75	0.99	12.93	0.99	6.40	**0.02**	4.43	0.65	14.56	0.79	3.87	0.06	0.14	1.00	2.25	0.15	30.40	**<0.01**
Transect	20.20	**0.05**	2.97	0.99	6.03	0.14	0.96	0.40	0.09	0.92	10.34	0.09	0.83	0.45	14.89	0.06	1.88	0.18	1.50	0.23
Elevation*Transect	28.02	**0.03**	2.43	0.99	7.46	0.12	0.92	0.42	0.21	0.82	8.81	0.10	0.66	0.53	13.06	0.07	1.77	0.20	0.77	0.47

	cPOM + fPOM				Silt & clay fraction / MAOM										DOC			
	Contribution of fractions to total SOC *		SOC stock*		Mass*		SOC concentration *		Contribution of MAOM to total SOC *		SOC stock*		C/N ratio*		SOC stock*		C/N ratio*	
Statistic	F	p	F	p	F	p	F	p	F	p	F	p	F	p	F	p	F	p
Elevation	9.11	0.44	30.03	0.91	12.17	1.00	59.99	1.00	9.07	0.27	8.43	0.34	6.26	0.13	4.68	**0.03**	30.40	**<0.01**
Transect	4.47	0.18	0.59	0.96	4.68	0.18	1.17	0.46	4.49	0.18	0.11	0.90	0.53	0.65	0.61	0.55	1.50	0.23
Elevation*Transect	6.32	0.14	0.50	0.96	6.12	0.14	0.89	0.53	6.34	0.14	0.41	0.71	0.79	0.56	0.00	1.00	0.77	0.47

	cPOM + fPOM + MAOM									
	Mass		SOC concentration		Contribution of fractions to total SOC		SOC stock*		C/N ratio	
Statistic	F	p	F	p	F	p	F	p	F	p
Elevation	0.00	0.98	10.28	**<0.01**	0.02	0.90	1.53	0.23	10.69	**<0.01**
Transect	0.11	0.90	0.98	0.39	0.02	0.98	0.40	0.68	1.05	0.37
Fraction	11.81	**<0.01**	5.12	**0.01**	2.90	0.06	1.65	0.21	4.74	**0.02**
Elevation*Transect	0.14	0.87	0.77	0.48	0.02	0.98	0.80	0.47	0.76	0.48
Elevation*Fraction	4.33	**0.02**	2.49	0.10	3.38	**0.04**	0.12	0.88	3.10	0.07
Transect*Fraction	4.35	**<0.01**	1.00	0.43	2.86	**0.03**	0.63	0.65	1.83	0.17
Elevation*Transect*Fraction	5.74	**<0.01**	0.88	0.49	3.29	**0.02**	1.12	0.36	1.50	0.24

5 Discussion

In general, bulk soil organic carbon [SOC] stocks, as well as soil respiration [SR] and standardized SR at 10°C [SR_{10}] increase with decreasing elevation across the entire transects as well as across the sites above the treeline. With respect to parent material, SR is on average two times higher on calcareous than on siliceous parent material. Also, SR_{10} is higher on calcareous sites when looking at the entire transect length but not for the sites above the treeline. In contrast to SR, only few parameters measured within the fractions show elevation-relevant trends, whereby the influence of the parent material shows no linear pattern.

5.1 Elevational trends

5.1.1 Bulk soil organic carbon stocks

Bulk SOC stocks at a depth of 0 – 10 cm increase with decreasing elevation, supporting the first hypothesis. However, SOC stocks do not increase linearly with decreasing elevation across the transects: Grassland sites show the highest SOC stocks in each transect (average 2.4 kg C m^{-2}), while the higher situated nival sites (cushion plants, sparse vegetation, and vegetation-free) show comparatively very small stocks (average 0.3 kg C m^{-2}). Forest and shrub sites generally show higher values (average 1.8 kg C m^{-2}) than nival sites but lower values than grassland sites. These results are consistent with other gradient studies: Early successional ecosystems in the nival zone show very low SOC stocks due to low plant inputs (Smittenberg et al., 2012). Feyissa et al. (2023) observed higher SOC stocks in alpine grasslands than in forests at lower elevations. Also, Badraghi et al. (2021) found that SOC increased with decreasing elevation.

In general, SOC stocks depend on litter productivity, which is linked to the type of vegetation (Djukic et al., 2010) and the extent of litter decomposition (Ohtonen et al., 1999; Zollinger et al., 2013). Perruchoud et al. (1999) also argued that increased biomass production and the associated greater input of organic matter into the soil will increase SOC stocks. As vegetation productivity generally increases with decreasing elevation (Leifeld et al., 2009), SOC stocks should show similar patterns (Zollinger et al., 2013). The increased weathering of parent rock and associated increased soil formation (Musso et al., 2022) could further explain the increased SOC stocks in the topsoil with decreasing elevation. In grasslands, SOC is mainly stored in the mineral horizons (Khedim et al., 2023), while a large proportion of organic C in coniferous forests is stored in thick organic layers due to the poor degradability of plant litter (Faggian et al., 2012; Canedoli et al., 2020). Therefore, topsoil samples from grassland sites show higher SOC stocks than those from forest sites, as a considerable amount of the SOC in forest sites is stored in the organic layer, which was not considered in this work. In addition, fine root input and microbial necromass is usually higher in topsoils in grasslands than in forests which represent considerable C deposits (Hiltbrunner et al., 2013; Bai & Cotrufo, 2022).

The harsher climate in grassland sites may further lead to reduced decomposition rates, which in turn favors the accumulation of SOC in the topsoil of grassland sites (Djukic et al., 2010; Khedim et al., 2023). Overall, SOC stocks within the first 10 cm of soil increase with decreasing elevation, probably due to a complex interplay of above and belowground plant C input through an increasing vegetation cover and increased soil formation with decreasing elevation.

5.1.2 Soil fractions

Weathering of parent material generally increases with decreasing elevation (von Lützow et al., 2007; Mikutta et al., 2009). Mainka et al. (2022) observed an increase in mineral-associated organic matter [MAOM] with increasing soil weathering as more reactive mineral surfaces are available to form MAOM (Creamer et al., 2019). For this study, it was therefore assumed that the contribution of mineral-associated organic C [MAOC] to bulk SOC stocks would behave similarly as there are more mineral surfaces available for organic carbon to bind to with decreasing elevation. However, this was not the case: The contribution of MAOC to total SOC does not increase with decreasing elevation. Therefore, the second hypothesis must be rejected.

Egli et al. (2014) state that weathering rates decrease with time, which could possibly explain the non-linear contribution of MAOC to the total SOC stocks along the gradients. Moreover, the proportion of MAOM is usually higher in deeper soil layers (Leifeld et al., 2009; Mainka et al., 2022). Hence, elevation and thus weathering dependent trends of proportions of MAOC to total SOC may not be present in the topsoil to which the particle size fractionation was limited in this study.

Grassland sites generally show the highest MAOC stocks in the topsoil. The high MAOC stocks in topsoils of grassland sites may be linked to the high input by fine roots (Hiltbrunner et al., 2013; Bramble et al., 2024) and to large amounts of microbial necromass (Bai & Cotrufo, 2022). Coarse particulate organic carbon [cPOC] stocks increase linearly with decreasing elevation in topsoils. Higher cPOC stocks might be related to an increasingly bad degradability and higher input of litter with decreasing elevation (Djukic et al., 2010). The linear increase in C/N ratio of bulk topsoil samples reinforces this assumption. Lastly, the fractions' model showed that the SOC concentration in the fractions generally increases with decreasing elevation which goes along the general increase in SOC stocks of the bulk soil samples (see 5.1.1). Still, it remains unclear why there aren't any other elevational trends in the soil fractions as found in other gradient studies in alpine environments.

5.1.3 Soil respiration

Soil respiration increases with decreasing elevation in all transects, which aligns with the assumption in hypotheses 3. Egli & Poulenard (2016) argued that along an elevation gradient, mean temperatures generally increase with decreasing elevation which could also be associated with an enhanced decomposition (Zhao et al., 2017). In the present study, soil temperatures increase with decreasing elevation. However, SR_{10} also increases with decreasing elevation. Therefore, the measured soil

temperature may not be as relevant in controlling SR (e.g. Rodeghiero et al., 2005; Zhao et al., 2017) as the general increase in temperature with decreasing elevation described by Egli & Poulenard (2016). Although litter input was not investigated in the context of this thesis, C inputs are meant to increase with decreasing elevation due to higher vegetation cover and productivity (Perruchoud et al., 1999). Therefore, increasing C inputs and the enhanced SOC stocks with decreasing elevation could further explain the increase in SR with decreasing elevation.

Several studies (e.g. Raich and Schlesinger, 1992; Wang et al., 2017) have found higher decomposition rates with an increase in water content (Zhao et al., 2021). In this study, fine earth moisture also increases with decreasing elevation and could therefore be an explanatory variable for SR which can be restricted by low moisture contents (Hagedorn & Joos, 2014). Nevertheless, it seems unlikely that moisture was restricting SR in the present study as moisture contents are above critical values (Fang & Moncrieff, 2001; Guelland et al., 2013). Ultimately, the increase in SR with decreasing elevation can likely be explained by warmer temperatures, an enhanced plant productivity, and greater SOC stocks.

5.2   Effects of the parent material

5.2.1   Bulk soil organic carbon stocks

Based on the findings of Musso et al. (2022), it was assumed that the higher weathering rates of siliceous parent material would lead to faster soil formation. This would go along with greater SOC stocks on siliceous compared to calcareous parent material. However, no significant differences in SOC stocks in the topsoil between calcareous and silicious sites are apparent. Therefore, the fourth hypothesis must be rejected.

Egli et al. (2014) concluded that the weathering rates of parent material decreases with time, which may offset any differences between parent materials. This is supported by Montagnani et al. (2019) who showed that SOC accumulation slowed down after 150 years. On the contrary, a master's thesis carried out in the same study area / project showed that the soils on calcareous parent materials are in general less developed (Marty, 2024). Nonetheless, Musso et al. (2022) argue that parent material may dominate soil formation and SOC accumulation in the early stages of development, while other factors such as vegetation become major drivers of soil formation over time. Site variability and different exposures of sites in the study area (Egli & Poulenard, 2016) as well as elevational trends, may outweigh the influence of parent material on SOC stocks of topsoils in the long term.

Still, the question arises why grassland sites in the gneissic transect (T3) show far higher SOC stocks than in the calcareous (T1) and amphibolitic transect (T2). In this regard, the accompanying master's thesis of Marty (2024) found the highest clay contents on gneissic parent material at those sites which can be linked to an increased stabilization of SOC as mineral surfaces are a prerequisite for the formation of MAOM (Leifeld et al., 2009; Cotrufo & Lavallee, 2022). Topsoils at those sites also show high shares of MAOM and MAOC stocks of up to 3 kg C m^{-2} and low pH values which would limit decomposition processes (Leifeld et al., 2009; Budge et al., 2011). Finally, differences between bulk SOC stocks in

topsoils of calcareous and siliceous sites are not apparent, while high SOC stocks in grassland sites on gneissic parent material can be related to favorable soil conditions and also show high shares of MAOM.

5.2.2 Soil fractions

Higher weathering and soil formation rates were found on siliceous parent material by Musso et al. (2022). It was therefore expected that the siliceous sites would have more mineral surface area and therefore higher proportions of MAOC to total SOC (Leifeld et al., 2009). However, this was not the case. Hence, the fifth hypothesis must be rejected.

As for the bulk SOC stocks, the impact of the parent material on the topsoil may be relatively small (Mainka et al, 2022) and could be more site dependent. Only the mass of cPOM differs significantly between the three transects. Here, the amphibolitic transect (T2) shows very high proportions of cPOM across the entire transect but especially in the nival sites above 2700 m where the SOC concentration within the cPOM is almost zero which would indicate a high proportion of inorganic matter. Moreover, clay contents are highest in gneissic grassland sites (Marty, 2024). This may be linked to an increased weathering of parent material at those sites and could explain the enhanced mass proportions of MAOM, MAOC stocks, and proportions of MAOC to total SOC on gneissic grassland sites (Mainka et al., 2022). However, it cannot be conclusively clarified why SOC pools within the fractions do not differ among parent materials in this thesis as found in other gradient studies.

5.2.3 Soil respiration

As soils on calcareous parent material were expected to be less developed and contain higher stocks of particulate organic carbon [POC] and thus more labile C (Mikutta et al., 2009; Prietzel & Christophel, 2014; Musso et al., 2022), SR was predicted to be higher on calcareous than on siliceous parent material. In fact, average SR was more than twice as high on calcareous parent material than on siliceous parent material. However, there was no significant difference in POC stocks between parent materials which would have provided a straightforward explanation for the increased SR on calcareous rock. Therefore, the sixth hypothesis can only be partially accepted.

Pan et al. (2024) also found proportions of POC to be similar among different parent materials. They concluded that sufficient input of organic matter by plants and generally slow decomposition rates due to the cold climate outweigh the potential influence of the parent material (Pan et al., 2024). Furthermore, Prietzel & Christophel (2014) argue that the parent material has a stronger influence on SOM with increasing soil depth. This is supported by the findings of the accompanying master thesis which revealed that parent material affects SOM stocks in the deeper soil (Marty, 2024). Parent material may not be of great importance for the accumulation of POM and thus the amount of POC in the topsoil. Looking at topsoil pH, the values on calcareous parent material are consistently higher. Surprisingly, the model did not identify the pH values of topsoils to be significantly different between calcareous and siliceous sites. But higher pH can be decisive for SR as microbial activity and decomposition is usually

lower in soils with low pH values (Leifeld et al., 2009; Budge et al., 2011; Speckert & Wiesenberg, 2023) which could explain the enhanced SR on calcareous compared to siliceous sites. Conclusively, SR is higher on calcareous than on siliceous parent material. However, it cannot be explained by looking at POC stocks. Topsoil pH or other variables which have not been investigated in the frame of this thesis may be more decisive in characterizing SR among different parent materials.

5.3   Soil organic carbon vulnerability

Hagedorn et al. (2019) state that future warming may provoke an upward vegetation shift by 300 – 600 m in elevation. Such a change in flora will ultimately alter the amount of litter and its quality (Hitz et al., 2001). Treeline advancement often results in an accumulation of an organic layer (Hiltbrunner et al., 2013) in which SOC is stored in labile SOM which is more vulnerable to be lost to the atmosphere (Hagedorn et al., 2010b; Hagedorn et al., 2019). Warming may lead to an increased input through an enhanced litter production but also to higher respiratory losses in the soil as higher temperatures promote the activity of microbial communities (Hagedorn et al., 2010a; Donhauser et al., 2021). Hitz et al. (2001) state that the shift in vegetation usually occurs slower than the rise in temperature. Therefore, Hagedorn et al. (2019) suggest that SOC will be lost to the atmosphere. Yet differences in terms of climatic stability between POM and MAOM are crucial here (Rocci et al., 2020, Lugato et al., 2021):

In the topsoils of this study, between 55 – 88% of the bulk SOC stock is stored as MAOC while POC contributes to 12 – 45% of the bulk SOC stock. Compared to other studies, POC values are much lower (e.g. Budge et al., 2011; Hagedorn et al, 2019). This poses the question whether parts of the MAOM could possibly belong to the POM. This assumption is reinforced through the relatively high C/N values of the MAOM fraction. While C/N values in the POM fraction are generally consistent with present studies, the C/N ratios in the MAOM are mostly higher (von Lützow et al., 2007; Cotrufo et al., 2019). This might be influenced by shares of POM in the MAOM. It is therefore assumed that there may be more POM and thus labile C in the soil than the data could reveal. Hence, more SOC than was described here may be vulnerable to changing climatic conditions and could be lost to the atmosphere, promoting global warming (Hagedorn et al., 2019; Khedim et al., 2023). However, it is not feasible to estimate the extent and time span of SOC loss to the atmosphere within the scope of this study. Finally, differences in C stocks and fluxes among parent materials were found, but its mechanisms and drivers cannot be clearly assessed in the frame of this study. Hence, the influence of the parent material on the stability of SOC under future warming scenarios remains unresolved.

6 Uncertainties & limitations

Although this study is based on methods derived from scientific literature, several difficulties and uncertainties arose during the field work, sampling procedure, laboratory part and data analysis.

6.1 Study area

Mountain soils are extremely diverse and contain an extreme spatial variability (Baruck et al., 2016; Pintaldi et al., 2021). This is also true for this study area: Although the three transects are relatively close to one another (especially T2 & T3), the 28 sites are characterized by many different conditions with different geology, aspect, slope gradient, vegetation cover, and geomorphology. Additionally, the transects' lengths and elevation ranges differ strongly. On top of that, the amphibolitic transect (T2) also contains gneissic parent material which could affect the outcome of the study. Thus, the site heterogeneity within the study area may alter the outcome of the study.

6.2 Field work

Although the field work was precariously planned, difficulties during the realization arose: The site FS2000 on the amphibolitic transect (T2) could not be sampled in July as we did not have the authorization to drive to that location. Soil respiration [SR] measurements in August on the gneissic transect (T3) were unreasonably high compared to July and September and were not used for the analysis as they distorted the results.

At the sites FS3040, FS3100 and IB2800, SR measurements were conducted using a 3 m x 3 m tarp. This approach was chosen because SR at high elevations is generally low (e.g. Badraghi et al., 2021; Zhao et al., 2017; Guo et al., 2022) and it was not possible to set the measurement chamber airtight on the ground. However, a comparison with standalone chambers at other high alpine sites as well as grassland soils during the winter was able to show a good correlation between the two methods (Udke, 2023: see 7.2.1). Air pressure was approximated in only three steps according to the elevation of the site. Yet it remains unclear, whether the results of the applied SR measurement method are comparable with other studies (Rodeghiero et al., 2005) which used more standardized methods (e.g. *LI-COR* used by Grand et al., 2016; Badraghi et al., 2021). Soil respiration has been measured at the surface, while most variables have been measured / calculated for a range of 0-10 cm. Moreover, SR includes the heterotrophic carbon dioxide [CO_2] emission from the soil in the form of decomposing soil organic matter [SOM] as well as the autotrophic CO_2 emission from the roots throughout the whole soil body (Badraghi et al., 2021). It is therefore questionable whether the topsoil parameters help to explain SR even though the upper most soil layers are the most actives (Weldmichael et al., 2020). Still, the soil layers beneath 10 cm will also influence SR as soil organic carbon [SOC] is also stored in deeper soil depth but in smaller concentrations (Dinakaran et al., 2018).

6.3 Lab work

Some uncertainties and inaccuracies also arose during the particle size fractionation which may have had influences on the negative mass balance in the end (see 3.2.2.5). Especially during wet sieving, but also during the sonification and decanting steps, soil material has been lost in smaller proportions. Moreover, the methods had to be slightly adapted during the fractionation procedure due to time constraints and lack of equipment. However, it is unclear how much material has been lost during which step in the procedure. Furthermore, the fumigation procedure of the calcareous samples has been bypassed by using the $\delta^{13}C$ values which is why the proportions of SOC might be slightly incorrect for the SOC pools in T1.

As already mentioned in the discussion (see 5.3), the weight shares of particulate organic matter [POM] are lower and weight shares of mineral-associated organic matter [MAOM] are higher than in other gradient studies. An additional fractionation step or a different fractionation procedure (e.g. density fractionation) could lead to a better distinction of SOM and would be more comparable to other studies (e.g. Budge et al., 2011). In the end, the fractionation dataset was rather incomplete due to excessively high or low initial weights. Therefore, the dataset had to be completed with previously assessed results of the XThaw project which reduces the accuracy of the fractionation.

6.4 Data quality & Model design

For the models, several assumptions were made: Elevation has been taken as a proxy for temperature and vegetation while transect represents parent material and topography within the study area. Furthermore, most residuals were non-normally distributed due to the nature of data for a large part of response variables. However, most Shapiro tests rejected the Null hypothesis of normally distributed residuals only slightly and the residuals in the Q-Q plot often aligned on a line which was relatively straight. Still, the non-compliance with the normally distributed residuals weakens the validity of the study.

The primary constraint may however lie in conducting advanced statistics on a very limited dataset. Moreover, the sites have been measured only three times during Summer 2023 which raises the question of how representative the collected data is. Other studies also looked at different parameters which could have influenced the results of this thesis as well. However, as the chosen duration of this work was restricted, the (data) analysis had to be limited to the present selection of variables.

7   Conclusion & Outlook

It has been shown that soil organic carbon [SOC] stocks in the topsoil (0 – 10 cm) increase with decreasing elevation possibly related to an enhanced input of carbon [C] due to greater vegetation cover and productivity. Proportions of mineral-associated organic carbon [MAOC] to total SOC do not increase as expected with decreasing elevation. However, MAOC stocks are greatest in grassland sites strongly suggesting large amounts of stable SOC. Reason for this could be the enhanced productivity of fine roots and the abundance of microbial necromass in these topsoils. Soil respiration [SR] increases with decreasing elevation and can possibly be linked to a general increase in temperature, higher SOC stocks, and an enhanced productivity of vegetation.

Parent material has strong effects on SR but only minor effects on C pools: Soil respiration is on average two times higher on calcareous than on siliceous parent material. The increased SR on calcareous parent material can likely be explained by the microbial productivity which is promoted by the consistently higher pH values of the calcareous sites. Grassland soils between 2000 and 2500 m on gneissic parent material have the highest bulk SOC and MAOC stocks. Yet there are no differences in bulk SOC stocks and C pools within the physical soil fractions among parent materials.

It can be concluded that the influence of parent material on alpine topsoil C pools and fluxes remains partially unclear as it was not feasible to fully assess its mechanisms and drivers in the context of this study. Consequently, it remains uncertain how parent material influences SOC vulnerability under a warming climate.

Future studies should investigate how different parent materials affect C pools and fluxes in alpine areas by analyzing entire soil profiles and using a different fractionation method (e.g. density fractionation) which is more comparable to other studies. Research projects should also look at differences between autotroph & heterotroph respiration, and monitoring should be performed over longer time periods to be able to make more accurate statements about the changing C fluxes in alpine soils under future climate change.

8 Appendix

8.1 Sources

8.1.1 Literature

Amelung, W., Flach, K.-W., & Zech, W. (1999). Lignin in Particle-Size Fractions of Native Grassland Soils as Influenced by Climate. Soil Science Society of America Journal, 63(5), 1222–1228. https://doi.org/10.2136/sssaj1999.6351222x

Angst, G., Messinger, J., Greiner, M., Häusler, W., Hertel, D., Kirfel, K., Kögel-Knabner, I., Leuschner, C., Rethemeyer, J., & Mueller, C. W. (2018). Soil organic carbon stocks in topsoil and subsoil controlled by parent material, carbon input in the rhizosphere, and microbial-derived compounds. Soil Biology and Biochemistry, 122(April), 19–30. https://doi.org/10.1016/j.soilbio.2018.03.026

Badraghi, A., Ventura, M., Polo, A., Borruso, L., Giammarchi, F., & Montagnani, L. (2021). Soil respiration variation along an altitudinal gradient in the Italian Alps: Disentangling forest structure and temperature effects. PLoS ONE, 16(8 August), 1–20. https://doi.org/10.1371/journal.pone.0247893

Bai, Y., & Cotrufo, M. F. (2022). Grassland soil carbon sequestration: Current understanding, challenges, and solutions. Science, 608(August), 603–608.

Baruck, J., Nestroy, O., Sartori, G., Baize, D., Traidl, R., Vršcaj, B., Bräm, E., Gruber, F. E., Heinrich, K., & Geitner, C. (2016). Soil classification and mapping in the Alps: The current state and future challenges. Geoderma, 264, 312–331. https://doi.org/10.1016/j.geoderma.2015.08.005

Batjes, N. H. (1996). Total carbon and nitrogen in the soils of the world. European Journal of Soil Science, 47(2), 151–163. https://doi.org/https://doi.org/10.1111/j.1365-2389.1996.tb01386.x

Bird, M., Santùckoá, H., Lloyd, J., Veenedaal, E., (2001). Global soil organic carbon pool. In: Schulze, E.D., Heimann, M., Harrison, S., Holland, E., Lloyd, J., Prentice, I.C., Schimel, D. (Eds.), Global Biogeochemical Cycles in the Climate System. Academic Press, San Diego, pp. 185-199.

Bockheim, J. G., & Munroe, J. S. (2014). Organic carbon pools and genesis of alpine soils with permafrost: A review. Arctic, Antarctic, and Alpine Research, 46(4), 987–1006. https://doi.org/10.1657/1938-4246-46.4.987

Bramble, D. S. E., Ulrich, S., Schöning, I., Mikutta, R., Brandt, L., Poll, C., Kandeler, E., Mikutta, C., Konrad, A., Siemens, J., Yang, Y., Polle, A., Schall, P., Ammer, C., Kaiser, K., Schrumpf, M. (2024). Formation of mineral-associated organic matter in temperate soils is primarily controlled by mineral

type and modified by land use and management intensity. Global Change Biology, 30(1). https://doi.org/10.1111/gcb.17024

Budge, K., Leifeld, J., Hiltbrunner, E., & Fuhrer, J. (2011). Alpine grassland soils contain large proportion of labile carbon but indicate long turnover times. Biogeosciences, 8(7), 1911–1923. https://doi.org/10.5194/bg-8-1911-2011

Canedoli, C., Ferrè, C., Abu El Khair, D., Comolli, R., Liga, C., Mazzucchelli, F., Proietto, A., Rota, N., Colombo, G., Bassano, B., Viterbi, R., & Padoa-Schioppa, E. (2020). Evaluation of ecosystem services in a protected mountain area: Soil organic carbon stock and biodiversity in alpine forests and grasslands. Ecosystem Services, 44(January). https://doi.org/10.1016/j.ecoser.2020.101135

Cotrufo, M. F., Ranalli, M. G., Haddix, M. L., Six, J., & Lugato, E. (2019). Soil carbon storage informed by particulate and mineral-associated organic matter. Nature Geoscience, 12(12), 989–994. https://doi.org/10.1038/s41561-019-0484-6

Cotrufo, M. F., & Lavallee, J. M. (2022). Soil organic matter formation, persistence, and functioning: A synthesis of current understanding to inform its conservation and regeneration. In Advances in Agronomy, 172(1), 1-66 Elsevier Inc. https://doi.org/10.1016/bs.agron.2021.11.002

Creamer, C. A., Foster, A. L., Lawrence, C., McFarland, J., Schulz, M., & Waldrop, M. P. (2019). Mineralogy dictates the initial mechanism of microbial necromass association. Geochimica et Cosmochimica Acta, 260, 161–176. https://doi.org/10.1016/j.gca.2019.06.028

Dinakaran, J., Chandra, A., Chamoli, K. P., Deka, J., & Rao, K. S. (2018). Soil organic carbon stabilization changes with an altitude gradient of land cover types in central Himalaya, India. Catena, 170(June), 374–385. https://doi.org/10.1016/j.catena.2018.06.039

Djukic, I., Zehetner, F., Tatzber, M., & Gerzabek, M. H. (2010). Soil organic-matter stocks and characteristics along an alpine elevation gradient. Journal of Plant Nutrition and Soil Science, 173(1), 30–38. https://doi.org/10.1002/jpln.200900027

Donhauser, J., Qi, W., Bergk-Pinto, B., & Frey, B. (2021). High temperatures enhance the microbial genetic potential to recycle C and N from necromass in high-mountain soils. Global Change Biology, 27(7), 1365–1386. https://doi.org/10.1111/gcb.15492

Dutta, H., & Dutta, A. (2016). The microbial aspect of climate change. Energy, Ecology and Environment, 1(4), 209–232. https://doi.org/10.1007/s40974-016-0034-7

Egli, M., Dahms, D., & Norton, K. (2014). Soil formation rates on silicate parent material in alpine environments: Different approaches-different results? Geoderma, 213, 320–333. https://doi.org/10.1016/j.geoderma.2013.08.016

Egli, M., & Poulenard, J. (2016). Soils of Mountainous Landscapes. International Encyclopedia of Geography, 1–10. https://doi.org/10.1002/9781118786352.wbieg0197

Eswaran, H., Van Den Berg, E., & Reich, P. (1993). Organic Carbon in Soils of the World. Soil Science Society of America Journal, 57(1), 192–194. https://doi.org/https://doi.org/10.2136/sssaj1993.03615995005700010034x

Faggian, V., Bini, C., & Zilioli, D. M. (2012). Carbon stock evaluation from topsoil of forest stands in ne Italy. International Journal of Phytoremediation, 14(4), 415–428. https://doi.org/10.1080/15226514.2011.620656

Fang, C., & Moncrieff, J. B. (2001). The dependence of soil CO2 efflux on temperature. Soil Biology and Biochemistry, 33(2), 155–165. https://doi.org/10.1016/S0038-0717(00)00125-5

Fetzer, J., Moiseev, P., Frossard, E., Kaiser, K., Mayer, M., Gavazov, K., & Hagedorn, F. (2024). Plant–soil interactions alter nitrogen and phosphorus dynamics in an advancing subarctic treeline. Global Change Biology, 30(3), e17200. https://doi.org/10.1111/gcb.17200

Feyissa, A., Raza, S. T., & Cheng, X. (2023). Soil carbon stabilization and potential stabilizing mechanisms along elevational gradients in alpine forest and grassland ecosystems of Southwest China. Catena, 229(April), 107210. https://doi.org/10.1016/j.catena.2023.107210

Gavazov, K., Ingrisch, J., Hasibeder, R., Mills, R. T. E., Buttler, A., Gleixner, G., Pumpanen, J., & Bahn, M. (2017). Winter ecology of a subalpine grassland: Effects of snow removal on soil respiration, microbial structure and function. Science of the Total Environment, 590–591, 316–324. https://doi.org/10.1016/j.scitotenv.2017.03.010

Gobiet, A., Kotlarski, S., Beniston, M., Heinrich, G., Rajczak, J., & Stoffel, M. (2014). 21st century climate change in the European Alps-A review. Science of the Total Environment, 493, 1138–1151. https://doi.org/10.1016/j.scitotenv.2013.07.050

Grand, S., Rubin, A., Verrecchia, E. P., & Vittoz, P. (2016). Variation in soil respiration across soil and vegetation types in an Alpine valley. PLoS ONE, 11(9), 1–16. https://doi.org/10.1371/journal.pone.0163968

Green, C., & Byrne, K. A. (2004). Biomass: Impact on carbon cycle and greenhouse gas emissions. Encyclopedia of Energy, 223–236. https://doi.org/DOI:10.1016/B0-12-176480X/00418-6

Gubler, A., Gross, T., Hug, A.-S., Moll-Mielewczik, J., Müller, M., Rehbein, K., Schwab, P., Wächter, D., Zimmermann, R., & Meuli, R. G. (2022). Die Nationale Bodenbeobachtung 2021. https://doi.org/10.34776/as128g

Guelland, K., Hagedorn, F., Smittenberg, R. H., Göransson, H., Bernasconi, S. M., Hajdas, I., & Kretzschmar, R. (2013). Evolution of carbon fluxes during initial soil formation along the forefield of Damma glacier, Switzerland. Biogeochemistry, 113(1–3), 545–561. https://doi.org/10.1007/s10533-012-9785-1

Guidi, C., Lehmann, M. M., Meusburger, K., Saurer, M., Vitali, V., Peter, M., Brunner, I., & Hagedorn, F. (2023). Tracing sources and turnover of soil organic matter in a long-term irrigated dry forest using a novel hydrogen isotope approach. Soil Biology and Biochemistry, 184(July), 109113. https://doi.org/10.1016/j.soilbio.2023.109113

Guo, M., Zhao, B., Wen, Y., Hu, J., Dou, A., Zhang, Z., Rui, J., Li, W., Wang, Q., & Zhu, J. (2022). Elevational pattern of soil organic carbon release in a Tibetan alpine grassland: Consequence of quality but not quantity of initial soil organic carbon. Geoderma, 428(August). https://doi.org/10.1016/j.geoderma.2022.116148

Hagedorn, F., Spinnler, D., & Siegwolf, R. (2003). Increased N deposition retards mineralization of old soil organic matter. Soil Biology and Biochemistry, 35(12), 1683–1692. https://doi.org/10.1016/j.soilbio.2003.08.015

Hagedorn, F., Mulder, J., & Jandl, R. (2010a). Mountain soils under a changing climate and land-use. Biogeochemistry, 97(1), 1–5. https://doi.org/10.1007/s10533-009-9386-9

Hagedorn, F., Moeri, A., Walthert, L., & Zimmermann, S. (2010b). Kohlenstoff in Schweizer Waldböden – bei Klimaerwärmung eine potenzielle CO2-Quelle | Soil organic carbon in Swiss forest soils – a potential CO2 source in a warming climate. Schweizerische Zeitschrift fur Forstwesen, 161(12), 530–535. https://doi.org/10.3188/szf.2010.0530

Hagedorn, F., Martin, M., Rixen, C., Rusch, S., Bebi, P., Zürcher, A., Siegwolf, R. T. W., Wipf, S., Escape, C., Roy, J., & Hättenschwiler, S. (2010c). Short-term responses of ecosystem carbon fluxes to experimental soil warming at the Swiss alpine treeline. Biogeochemistry, 97(1), 7–19. https://doi.org/10.1007/s10533-009-9297-9

Hagedorn, F., & Joos, O. (2014). Experimental summer drought reduces soil CO2 effluxes and DOC leaching in Swiss grassland soils along an elevational gradient. Biogeochemistry, 117(2–3), 395–412. https://doi.org/10.1007/s10533-013-9881-x

Hagedorn F., Krause H.-M., Studer M., S. A., & A, G. (2018). Boden und Umwelt. In Nationales Forschungsprogramm «Nachhaltige Nutzung der Ressource Boden» (nfp 68) (Nummer 2). https://doi.org/10.1515/9783112586044

Hagedorn, F., Gavazov, K., & Alexander, J. M. (2019). Above- and belowground linkages shape responses ofmountain vegetation to climate change. Mountain Life, 365(September), 1119–1123.

Hagedorn, F., Mayer, M., Meusburger, K., Walthert, L., & Zimmermann, S. (2022). Organische Substanz in Schweizer Waldböden - eine wichtige, aber empfindliche Ressource. Waldböden - intakt und funktional.

Hiltbrunner, D., Zimmermann, S., & Hagedorn, F. (2013). Afforestation with Norway spruce on a subalpine pasture alters carbon dynamics but only moderately affects soil carbon storage. Biogeochemistry, 115(1–3), 251–266. https://doi.org/10.1007/s10533-013-9832-6

Hitz, C., Egli, M., & Fitze, P. (2001). Below-ground and above-ground production of vegetational organic matter along a climosequence in alpine grasslands. Journal of Plant Nutrition and Soil Science, 164(4), 389–574. https://doi.org/10.1002/1522-2624(200108)164:4<389::AID-JPLN389>3.0.CO;2-A

IPCC (2007). Summary for Policymakers. In: Climate Change 2007: The Physical Science Basis. Contribution of Working Group I to the Fourth Assessment Report of the Intergovernmental Panel on Climate Change [Solomon, S., D. Qin, M. Manning, Z. Chen, M. Marquis, K.B. Averyt, M.Tignor and H.L. Miller (eds.)]. Cambridge University Press, Cambridge, United Kingdom and New York, NY, USA.

IPCC (2023). Climate Change 2023: Synthesis Report. Contribution of Working Groups I, II and III to the Sixth Assessment Report of the Intergovernmental Panel on Climate Change [Core Writing Team, H. Lee and J. Romero (eds.)]. IPCC, Geneva, Switzerland.

Jobbagy, E. G., & Jackson, R. B. (2000). The Vertical Distribution of Soil Organic Carbon and Its Relation to Climate and Vegetation. Ecological Applications, 10(2), 423. https://doi.org/10.2307/2641104

Khedim, N., Poulenard, J., Cecillon, L., Baudin, F., Barre, P., Saillard, A., Bektas, B., Grigulis, K., Lavorel, S., Münkemüller, T., & Choler, P. (2023). Soil organic matter changes under experimental

pedoclimatic modifications in mountain grasslands of the French Alps. Geoderma, 429(January 2022). https://doi.org/10.1016/j.geoderma.2022.116238

Körner C. (2003). Alpine Plant Life: Functional Plant Ecology of High Mountain Ecosystems. Springer Berlin, Heidelberg.

Krull, E., Baldock, J., & Skjemstad, J. (2003). Importance of mechanisms and processes of the stabilisation of soil organic matter for modelling carbon turnover. Functional Plant Biology - FUNCT PLANT BIOL, 30. https://doi.org/10.1071/FP02085

Lavallee, J. M., Soong, J. L., & Cotrufo, M. F. (2019). Conceptualizing soil organic matter into particulate and mineral-associated forms to address global change in the 21st century. Global Change Biology, 26(1), 261–273. https://doi.org/10.1111/gcb.14859

Leifeld, J., Zimmermann, M., Fuhrer, J., & Conen, F. (2009). Storage and turnover of carbon in grassland soils along an elevation gradient in the Swiss Alps. Global Change Biology, 15(3), 668–679. https://doi.org/10.1111/j.1365-2486.2008.01782.x

Leupold, W., Eugster, H., Bearth, P., Spaenhauer, F., and Streckeisen, A., (1935). Geologischer Atlas der Schweiz 1:25'000, Blatt 423: Scaletta, Erläuterungen, A. Francke A.G., Bern.

Lugato, E., Lavallee, J. M., Haddix, M. L., Panagos, P., & Cotrufo, M. F. (2021). Different climate sensitivity of particulate and mineral-associated soil organic matter. Nature Geoscience, 14(5), 295–300. https://doi.org/10.1038/s41561-021-00744-x

Luo, Y., Wan, S., Hui, D., & Wallace, L. L. (2001). Acclimatization of soil respiration to warming in a tall grass prairie. Nature, 413(6856), 622–625. https://doi.org/10.1038/35098065

Maggetti, M., & Flisch, M. (1993). Evolution of the Silvretta Nappe. In J. F. von Raumer & F. Neubauer (Hrsg.), Pre-Mesozoic Geology in the Alps (S. 469–484). Springer Berlin Heidelberg. https://doi.org/10.1007/978-3-642-84640-3_28

Mainka, M., Summerauer, L., Wasner, D., Garland, G., Griepentrog, M., Berhe, A. A., & Doetterl, S. (2022). Soil geochemistry as a driver of soil organic matter composition: Insights from a soil chronosequence. Biogeosciences, 19(6), 1675–1689. https://doi.org/10.5194/bg-19-1675-2022

Marty, K. (2024). Carbon storage and vulnerability in alpine soils - soil organic matter changes across the treeline. Master's Thesis, Environmental System Science, Soil Resources, ETHZ.

Mikutta, R., Schaumann, G. E., Gildemeister, D., Bonneville, S., Kramer, M. G., Chorover, J., Chadwick, O. A., & Guggenberger, G. (2009). Biogeochemistry of mineral – organic associations across a long-term mineralogical soil gradient (0 . 3 – 4100 kyr), Hawaiian Islands. Geochimica et Cosmochimica Acta, 73(7), 2034–2060. https://doi.org/10.1016/j.gca.2008.12.028

Montagnani, L., Badraghi, A., Speak, A. F., Wellstein, C., Borruso, L., Zerbe, S., & Zanotelli, D. (2019). Evidence for a non-linear carbon accumulation pattern along an Alpine glacier retreat chronosequence in Northern Italy. PeerJ, 2019(10), 1–27. https://doi.org/10.7717/peerj.7703

Musso, A., Tikhomirov, D., Plötze, M. L., Greinwald, K., Hartmann, A., Geitner, C., Maier, F., Petibon, F., & Egli, M. (2022). Soil Formation and Mass Redistribution during the Holocene Using Meteoric10 Be, Soil Chemistry and Mineralogy. Geosciences (Switzerland), 12(2). https://doi.org/10.3390/geosciences12020099

Ohtonen, R., Fritze, H., Pennanen, T., Jumpponen, A., & Trappe, J. (1999). Ecosystem properties and microbial community changes in primary succession on a glacier forefront. Oecologia, 119(2), 239–246. https://doi.org/10.1007/s004420050782

Pan, Y., Ren, L., Huo, J., Xiang, X., Meng, D., Wang, Y., Yu, C., Liu, Y., Suo, J., & Huang, Y. (2024). Soil geochemistry prevails over root functional traits in controlling soil organic carbon fractions of the alpine meadow on the Qinghai-Tibet Plateau, China. Catena, 237(April 2023), 107814. https://doi.org/10.1016/j.catena.2024.107814

Pepin, N., Bradley, R. S., Diaz, H. F., Baraer, M., Caceres, E. B., Forsythe, N., Fowler, H., Greenwood, G., Hashmi, M. Z., Liu, X. D., Miller, J. R., Ning, L., Ohmura, A., Palazzi, E., Rangwala, I., Schöner, W., Severskiy, I., Shahgedanova, M., Wang, M. B., … Yang, D. Q. (2015). Elevation-dependent warming in mountain regions of the world. In Nature Climate Change (Bd. 5, Nummer 5, S. 424–430). https://doi.org/10.1038/nclimate2563

Perruchoud, D., Kienast, F., Kaufmann, E., & Bräker, O. U. (1999). 20th century carbon budget of forest soils in the Alps. Ecosystems, 2(4), 320–337. https://doi.org/10.1007/s100219900083

Pintaldi, Emanuele, D'Amico, M. E., Colombo, N., Colombero, C., Sambuelli, L., De Regibus, C., Franco, D., Perotti, L., Paro, L., & Freppaz, M. (2021). Hidden soils and their carbon stocks at high-elevation in the European Alps (North-West Italy). Catena, 198(105044). https://doi.org/10.1016/j.catena.2020.105044

Prietzel, J., & Christophel, D. (2014). Organic carbon stocks in forest soils of the German alps. Geoderma, 221–222, 28–39. https://doi.org/10.1016/j.geoderma.2014.01.021

Raich, J. W., & Schlesinger, W. H. (1992). The global carbon dioxide flux in soil respiration and its relationship to vegetation and climate. Tellus B, 44(2), 81–99. https://doi.org/10.1034/j.1600-0889.1992.t01-1-00001.x

Rebetez, M., & Reinhard, M. (2008). Monthly air temperature trends in Switzerland 1901-2000 and 1975-2004. Theoretical and Applied Climatology, 91(1–4), 27–34. https://doi.org/10.1007/s00704-007-0296-2

Rocci, K. S., Lavallee, J. M., Stewart, C. E., & Cotrufo, M. F. (2020). Soil organic carbon response to global environmental change depends on its distribution between mineral-associated and particulate organic matter: A meta-analysis. The Science of the total environment, 793, 148569. https://api.semanticscholar.org/CorpusID:236531032

Rodeghiero, M., & Cescatti, A. (2005). Main determinants of forest soil respiration along an elevation/temperature gradient in the Italian Alps. Global Change Biology, 11(7), 1024–1041. https://doi.org/10.1111/j.1365-2486.2005.00963.x

Rumpf, S. B., Gravey, M., Brönnimann, O., Luoto, M., Cianfrani, C., Mariethoz, G., & Guisan, A. (2022). vegetation productivity in the European Alps. Science, 1122(June), 1119–1122.

Sanderman, J., Amundson, R. G., & Baldocchi, D. D. (2003). Application of eddy covariance measurements to the temperature dependence of soil organic matter mean residence time. Global Biogeochemical Cycles, 17(2). https://doi.org/10.1029/2001gb001833

Scharlemann, J. P. W., Tanner, E. V. J., Hiederer, R., & Kapos, V. (2014). Global soil carbon: Understanding and managing the largest terrestrial carbon pool. Carbon Management, 5(1), 81–91. https://doi.org/10.4155/cmt.13.77

Schimel, D. S., Braswell, B. H., Holland, E. A., McKeown, R., Ojima, D. S., Painter, T. H., Parton, W. J., & Townsend, A. R. (1994). Climatic, edaphic, and biotic controls over storage and turnover of carbon in soils. Global Biogeochemical Cycles, 8(3), 279–293. https://doi.org/10.1029/94GB00993

Schlesinger, W. H. & Andrews, J. A. (2000). Soil Respiration and the Global Carbon Cycle. Biogeochemistry, 48(1), 7–20.

Simon, A., Geitner, C., & Katzensteiner, K. (2020). A framework for the predictive mapping of forest soil properties in mountain areas. Geoderma, 371(December 2019), 114383. https://doi.org/10.1016/j.geoderma.2020.114383

Sjögersten, S., Turner, B. L., Mahieu, N., Condron, L. M., & Wookey, P. A. (2003). Soil organic matter biochemistry and potential susceptibility to climatic change across the forest-tundra ecotone in the Fennoscandian mountains. Global Change Biology, 9(5), 759–772. https://doi.org/10.1046/j.1365-2486.2003.00598.x

Smittenberg, R. H., Gierga, M., Göransson, H., Christl, I., Farinotti, D., & Bernasconi, S. M. (2012). Climate-sensitive ecosystem carbon dynamics along the soil chronosequence of the Damma glacier forefield, Switzerland. Global Change Biology, 18(6), 1941–1955. https://doi.org/10.1111/j.1365-2486.2012.02654.x

Speckert, T. C., & Wiesenberg, G. L. B. (2023). Source or decomposition of soil organic matter: what is more important with increasing forest age in a subalpine setting? Frontiers in Forests and Global Change, 6, 0–15. https://doi.org/10.3389/ffgc.2023.1290922

Trautmann, S., Knoflach, B., Stötter, J., Elsner, B., Illmer, P., & Geitner, C. (2023). Potential impacts of a changing cryosphere on soils of the European Alps: A review. Catena, 232(June). https://doi.org/10.1016/j.catena.2023.107439

von Lützow, M., Kögel-Knabner, I., Ekschmitt, K., Flessa, H., Guggenberger, G., Matzner, E., & Marschner, B. (2007). SOM fractionation methods: Relevance to functional pools and to stabilization mechanisms. Soil Biology and Biochemistry, 39(9), 2183–2207. https://doi.org/10.1016/j.soilbio.2007.03.007

Wang, F., Peng, X., Wei, R., Qin, Y., & Zhu, X. (2019). Environmental behavior research in resources conservation and management: A case study of Resources, Conservation and Recycling. Resources, Conservation and Recycling, 141(November 2017), 431–440. https://doi.org/10.1016/j.resconrec.2018.10.024

Wackett, A. A., Yoo, K., Olofsson, J., & Klaminder, J. (2018). Human-mediated introduction of geoengineering earthworms in the Fennoscandian arctic. Biological Invasions, 20(6), 1377–1386. https://doi.org/10.1007/s10530-017-1642-7

Weldmichael, T. G., Michéli, E., Fodor, H., & Simon, B. (2020). The Influence of Depth on Soil Chemical Properties and Microbial Respiration in the Upper Soil Horizons. Eurasian Soil Science, 53(6), 780–786. https://doi.org/10.1134/S1064229320060137

XThaw, (2022). Project description. Swiss Federal Institute for Forest, Snow and Landscape Research [WSL] and the Institute for Snow and Avalanche Research [SLF].

Zhang, X., Li, M. J., Yang, C., Zhan, L. Q., Wu, W., & Liu, H. Bin. (2022). The stratification of soil organic carbon and total nitrogen affected by parent material and cropping system. Catena, 210(November 2021), 105898. https://doi.org/10.1016/j.catena.2021.105898

Zhao, J., Li, R., Li, X., & Tian, L. (2017). Environmental controls on soil respiration in alpine meadow along a large altitudinal gradient on the central Tibetan Plateau. Catena, 159(5), 84–92. https://doi.org/10.1016/j.catena.2017.08.007

Zhao, Y. F., Wang, X., Jiang, S. L., Zhou, X. H., Liu, H. Y., Xiao, J. J., Hao, Z. G., & Wang, K. C. (2021). Climate and geochemistry interactions at different altitudes influence soil organic carbon turnover times in alpine grasslands. Agriculture, Ecosystems and Environment, 320(July). https://doi.org/10.1016/j.agee.2021.107591

Zollinger, B., Alewell, C., Kneisel, C., Meusburger, K., Gärtner, H., Brandová, D., Ivy-Ochs, S., Schmidt, M. W. I., & Egli, M. (2013). Effect of permafrost on the formation of soil organic carbon pools and their physical-chemical properties in the Eastern Swiss Alps. Catena, 110, 70–85. https://doi.org/10.1016/j.catena.2013.06.010

8.1.2 Graphic content

If not declared differently, all graphic content was created by Cédric Bührer in the framework of this master's thesis.

Federal Office of Topography (Swisstopo) (2024). https://map.geo.admin.ch, accessed 11.01.2024.

Udke, A. (2023). Comparison of the two SR measurement methods: Chamber only vs tarp measurement.

8.1.3 Data

Federal Office of Meteorology and Climatology (MeteoSwiss) (2024). https://www.meteoswiss.admin.ch, accessed 17.01.2024.

Federal Office of Topography (Swisstopo) (2024). https://map.geo.admin.ch, accessed 11.01.2024.

Project XThaw (2022 – 2024).

Consult the table below for further information about the origin of the data.

Table 3: Listed data with the respective origin and method

Data	Origin	Method
CN, SOC in fractions	central lab WSL	See 3.2.3
Bulk CN, SOC	Project XThaw / central lab WSL	Element analysis & Isotope ratio mass spectrometry average from 0-10 cm off all replicates
Exposition	Project XThaw	GIS analysis in *ArcGIS* with a 2 m x 2 m DEM (Swisstopo)
Fine earth moisture	My own work	See 3.2.1
Parent material type	Project XThaw	Field observation / (maps.geo.admin.ch)
Particle size fractionation	My own work	See 3.2.2
Q10 / SR_{10}	My own work / Hagedorn et al. 2010c	See 3.3.2
Slope degree	Project XThaw	GIS analysis in *ArcGIS* with a 2 m x 2 m DEM (Swisstopo)
Soil respiration	My own work	See 3.1.2
Topsoil pH	Project XThaw	5g fine earth in 20ml 0.02M $CaCl_2$ (electrode) average from 0-10 cm off all replicates
Topsoil temperature	My own work	See 3.1.3
Vegetation	Project XThaw	Field observation / (maps.geo.admin.ch)
Volumetric soil moisture	My own work	See 3.1.4

8.2 Additional content

8.2.1 Plots

Tarp validation: comparison with chamber measurements
(WSL backyard + high alpine sites)
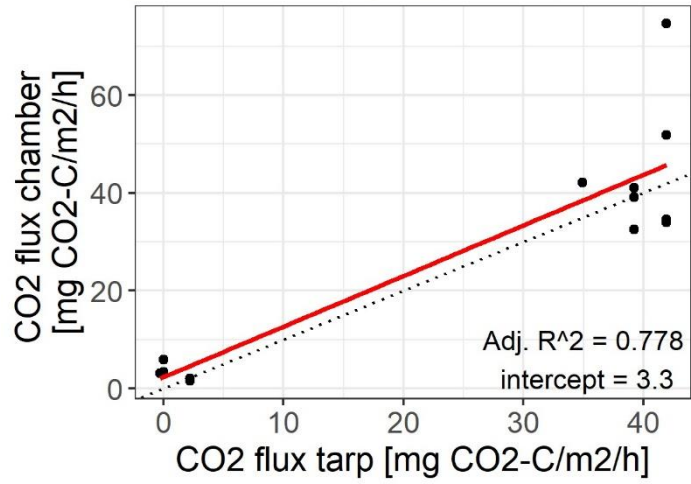
Figure 22: Comparison of the two SR measurement methods: Chamber only vs tarp measurement (Udke, 2023)

Model 1: Transect comparison, with all data and the subset of the sites above the treeline

```
lmer_soc                    <-lmer(SOC ~ Elevation * Transect_short +
(1|Location), data = data_all)
anova(lmer_soc)
qqnorm(residuals(lmer_soc))
shapiro.test(residuals(lmer_soc))


lmer_soc                    <-lmer(SOC ~ Elevation * Transect_short +
(1|Location), data = data_alpine)
anova(lmer_soc)
qqnorm(residuals(lmer_soc))
shapiro.test(residuals(lmer_soc))
```

Model 2: Bedrock comparison, with all data and the subset of the sites above the treeline

```
lmer_soc                    <-lmer(SOC ~ Elevation * Bedrock2 + (1|Location),
data = data_all)
anova(lmer_soc)
qqnorm(residuals(lmer_soc))
shapiro.test(residuals(lmer_soc))


lmer_soc                    <-lmer(SOC ~ Elevation * Bedrock2 + (1|Location),
data = data_alpine)
anova(lmer_soc)
qqnorm(residuals(lmer_soc))
shapiro.test(residuals(lmer_soc))
```

Model 3: Fractions' model, with the comparison of the transects and bedrock types

```
fractions_SOC_stock <-lmer(SOC_stock ~ Elevation*Transect_short*Fraction +
(1|Location), data=fractions)
anova(fractions_SOC_stock)
qqnorm(residuals(fractions_SOC_stock))
shapiro.test(residuals(fractions_SOC_stock))


fractions_SOC_stock <-lmer(SOC_stock ~ Elevation*Bedrock2*Fraction +
(1|Location), data=fractions)
anova(fractions_SOC_stock)
qqnorm(residuals(fractions_SOC_stock))
shapiro.test(residuals(fractions_SOC_stock))
```

Note that SOC/SOC stock have been selected as exemplary response variables to avoid having to depict

all variables. Data_all contains all sites while data_alpine excludes the sites with shrubs and forests.

Transect_short contains the three transects (T1, T2 & T3) while Bedrock2 contains either calcareous

or siliceous parent material.

8.2.3 Data

Table 4: Inneralpen – Büelenhorn transect (T1)

Site					Soil parameters				Measured variables during the field season				
Site / Elevation	Parent material	Vegetation	Exposition	Slope	pH	SOC	C/N	Month	ST	Fine earth moisture	Volumetric soil moisture	SR	SR_{10}
[m]	-	-	[°]	[°]	-	[kg m^2]	-	-	[°C]	[%]	[%]	[mg CO_2 m^{-2} h^{-1}]	[mg CO_2 m^{-2} h^{-1}]
IB2800	Calcareous	Cushion plants	27	15	6.9	NA	8.8	7	21.0	9.7	7.1	20.0	6.0
								8	2.1	22.0	8.4	5.2	12.3
								9	8.6	27.5	6.0	13.6	15.9
IB2750	Calcareous	Grassland	63	7	6.7	0.5	9.9	7	21.9	39.2	24.6	69.4	18.8
								8	5.3	44.0	21.8	45.3	75.7
								9	8.2	41.1	22.4	90.3	110.4
IB2570	Calcareous	Grassland	84	27	6.3	1.6	9.2	7	20.1	54.7	31.4	251.2	82.8
								8	7.8	67.8	36.3	162.2	206.6
								9	10.9	63.7	31.8	109.6	98.9
IB2340	Calcareous	Grassland	45	28	6.3	2.0	9.7	7	17.6	54.7	31.1	160.8	69.5
								8	10.7	59.6	45.3	192.1	177.3
								9	10.1	69.6	38.6	178.5	176.5
IB2180	Calcareous	Grassland	27	5	5.8	2.3	14.5	7	18.3	58.7	30.7	330.3	132.2
								8	13.2	62.1	41.7	253.8	179.2
								9	11.3	55.9	35.0	119.1	103.7
IB2000	Calcareous	Grassland	0	15	5.3	1.9	8.7	7	22.7	47.0	29.9	303.7	75.0
								8	14.5	59.9	39.4	240.2	146.5
								9	12.3	55.8	44.2	237.9	184.8
IB1970	Calcareous	Shrubs	8	21	6.9	1.9	27.2	7	15.0	61.2	11.9	285.1	165.2
								8	11.0	71.4	24.8	288.3	258.3
								9	10.7	73.6	22.5	159.4	148.1
IB1840	Calcareous	Forest	264	19	7.0	1.9	15.2	7	14.8	43.3	11.9	200.2	118.6
								8	9.7	65.7	33.1	190.9	198.0
								9	10.6	67.5	25.0	348.4	326.2

Table 5: Flüelapass – Schwarzhorn transect (T2)

Site					Soil parameters				Measured variables during the field season				
Site / Elevation	Parent material	Vegetation	Exposition	Slope	pH	SOC	C/N	Month	ST	Fine earth moisture	Volumetric soil moisture	SR	SR_{10}
[m]	-	-	[°]	[°]	-	[kg m^2]	-	-	[°C]	[%]	[%]	[mg CO_2 m^{-2} h^{-1}]	[mg CO_2 m^{-2} h^{-1}]
FS3100	Amphibolitic	None	112	16	4.9	0.2	10.5	7	16.8	22.4	0.0	16.8	8.0
								8	0.8	33.7	0.0	0.0	0.0
								9	4.7	25.9	0.0	0.0	0.0
FS3040	Amphibolitic	Sparse vegetation	129	19	4.4	0.1	10.1	7	26.4	10.4	3.7	8.5	1.4
								8	0.5	18.1	2.9	1.9	5.3
								9	14.7	11.7	4.1	11.9	7.1
FS2880	Amphibolitic	Cushion plants	244	20	4.6	0.3	10.9	7	20.5	21.5	7.3	153.5	48.6
								8	3.4	19.7	6.9	7.3	15.0
								9	3.1	17.1	6.5	8.1	17.3
FS2800	Amphibolitic	Cushion plants	27	10	4.5	NA	NA	7	27.1	14.7	6.7	14.8	2.3
								8	5.2	17.1	12.4	10.5	17.7
								9	14.5	16.6	9.8	7.9	4.8
FS2690	Amphibolitic	Grassland	52	21	4.2	1.2	13.9	7	19.4	40.9	30.2	103.1	36.6
								8	5.2	48.1	31.9	69.3	117.9
								9	10.6	45.8	27.6	57.1	53.3
FS2630	Amphibolitic	Grassland	129	21	4.0	1.8	13.7	7	20.7	48.6	33.7	254.4	78.2
								8	6.2	64.4	54.9	72.2	110.1
								9	13.4	55.7	30.0	249.4	172.3
FS2520	Amphibolitic	Grassland	135	36	4.1	2.3	13.0	7	18.2	33.7	20.8	264.8	108.0
								8	7.6	62.3	60.5	131.7	172.1
								9	17.4	57.3	26.9	214.6	94.9
FS2320	Amphibolitic	Grassland	45	4	3.5	1.7	14.5	7	21.2	45.3	20.2	96.8	28.2
								8	3.9	63.7	38.3	15.1	29.4
								9	12.1	56.8	27.5	124.1	98.9
FS2200	Amphibolitic / Gneissic	Shrubs	206	31	3.6	2.3	23.4	7	18.5	41.7	13.5	165.1	65.1
								8	5.5	45.1	35.0	41.0	67.0
								9	16.8	32.8	8.7	168.9	79.7
FS2000	Amphibolitic / Gneissic	Shrubs	116	22	4.4	1.7	15.9	7	NA	NA	NA	NA	NA
								8	10.7	84.8	58.8	63.4	58.5
								9	13.2	88.3	50.8	152.9	108.0
FS1830	Amphibolitic	Forest	200	34	4.7	1.5	17.5	7	14.3	61.7	8.1	149.0	92.9
								8	8.5	52.0	12.8	101.1	119.2
								9	11.6	65.2	4.2	264.6	221.1

Table 6: Dischmatal - Fuorcla Radönt transect (T3)

Site					Soil parameters				Measured variables during the field season				
Site / Elevation	Parent material	Vegetation	Exposition	Slope	pH	SOC	C/N	Month	ST	Fine earth moisture	Volumetric soil moisture	SR	SR_{10}
[m]	-	-	[°]	[°]	-	[kg m^2]	-	-	[°C]	[%]	[%]	[mg CO_2 m^{-2} h^{-1}]	[mg CO_2 m^{-2} h^{-1}]
DR2780	Gneissic	Cushion plants	191	13	4.1	0.7	13.6	7	16.3	25.7	10.7	34.3	17.1
								8	2.5	23.9	16.3	NA	NA
								9	5.0	21.6	15.5	16.4	28.3
DR2690	Gneissic	Grassland	180	15	3.7	2.5	16.7	7	10.1	54.9	56.8	12.9	12.8
								8	6.1	62.6	63.6	NA	NA
								9	10.0	58.2	49.5	15.4	15.5
DR2520	Gneissic	Grassland	162	4	3.7	5.3	14.8	7	13.7	54.8	68.0	39.2	26.2
								8	8.3	58.7	61.8	NA	NA
								9	11.5	59.2	52.8	35.0	29.7
DR2340	Gneissic	Grassland	211	15	3.7	3.0	15.8	7	16.9	60.2	28.4	62.8	29.3
								8	11.0	60.0	47.0	NA	NA
								9	12.2	47.0	34.6	73.0	57.1
DR2180	Gneissic	Grassland	242	10	3.5	3.1	14.9	7	17.6	52.4	44.6	75.1	32.6
								8	10.6	62.3	46.6	NA	NA
								9	12.4	58.9	52.1	20.6	15.7
DR2000	Gneissic	Grassland	270	5	3.3	4.3	21.6	7	18.3	70.1	94.8	29.7	12.0
								8	8.1	64.0	62.6	NA	NA
								9	14.3	67.3	52.1	28.5	17.8
DR1900	Gneissic	Shrubs	213	33	4.4	1.7	17.2	7	15.0	65.9	18.4	29.0	16.7
								8	10.8	59.8	23.5	NA	NA
								9	12.9	57.9	11.9	94.0	68.6
DR1820	Gneissic	Forest	259	24	4.2	2.1	11.7	7	14.6	59.2	25.3	70.0	42.2
								8	10.1	57.4	27.1	NA	NA
								9	10.6	59.1	22.6	15.8	14.9
DR1750	Gneissic	Forest	297	18	3.4	1.9	22.9	7	15.0	69.5	14.8	59.5	34.5
								8	9.8	62.9	22.7	NA	NA
								9	11.2	70.5	27.0	57.5	50.4

Table 7: cPOM + fPOM fractions

Location	Coarse sand fraction / cPOM					Fine sand fraction / fPOM					cPOM + fPOM	
	Mass	SOC concentration	Contribution of fractions to total SOC	SOC stock	CN	Mass	SOC concentration	Contribution of fractions to total SOC	SOC stock	C/N ratio	Contribution of fractions to total SOC	SOC stock
	[g]	[%C]	[%C]	[kg C m^{-2}]	-	[g]	[%C]	[%C]	[kg C m^{-2}]	-	[%C]	[kg C m^{-2}]
IB2800	6.4	NA	NA	NA	NA	9.3	0.6	NA	NA	NA	NA	NA
IB2750	3.4	2.1	6.0	0.0	NA	9.7	3.9	32.0	0.2	20.7	37.9	0.2
IB2570	2.9	NA	25.1	0.4	NA	6.5	8.0	15.9	0.3	20.5	41.0	0.7
IB2340	3.6	12.3	13.3	0.3	24.0	5.9	3.0	5.4	0.1	NA	18.7	0.4
IB2180	3.0	15.6	11.4	0.3	16.6	6.0	12.3	18.1	0.4	27.0	29.6	0.7
IB2000	3.3	1.6	1.8	0.0	NA	5.6	5.7	10.9	0.2	18.9	12.7	0.2
IB1970	4.1	NA	27.2	0.5	NA	5.6	27.3	17.2	0.3	36.6	44.4	0.8
IB1840	3.7	22.1	18.4	0.4	40.4	7.7	11.6	19.9	0.4	41.6	38.3	0.7
FS3100	16.6	NA	17.5	0.0	7.3	8.3	0.3	10.9	0.0	9.7	28.5	0.1
FS3040	14.7	NA	NA	NA	NA	10.6	NA	NA	NA	NA	33.2	0.0
FS2880	19.7	NA	NA	NA	NA	5.4	NA	NA	NA	NA	NA	NA
FS2800	17.4	0.1	13.5	NA	NA	6.3	0.3	18.1	NA	NA	31.6	NA
FS2690	12.9	0.9	10.5	0.1	NA	6.5	1.9	10.9	0.1	17.7	21.4	0.2
FS2630	7.4	4.3	14.0	0.2	16.4	6.9	3.4	10.3	0.2	NA	24.3	0.4
FS2520	8.6	5.6	11.1	0.3	17.5	6.5	12.5	18.8	0.4	16.7	29.9	0.7
FS2320	11.5	6.1	24.9	0.4	16.8	6.6	6.3	14.7	0.3	16.8	39.6	0.7
FS2200	8.7	4.9	14.6	0.3	13.3	7.9	8.5	23.1	0.5	28.6	37.7	0.9
FS2000	9.3	NA	NA	NA	NA	8.6	2.8	NA	NA	NA	NA	NA
FS1830	9.9	1.9	12.4	0.2	NA	9.4	3.0	27.3	0.4	NA	39.7	0.6
DR2780	8.1	NA	9.3	0.1	NA	7.6	0.5	7.2	0.1	NA	16.5	0.1
DR2690	6.9	NA	NA	NA	NA	6.4	NA	NA	NA	NA	NA	NA
DR2520	5.2	1.9	2.9	0.2	18.4	6.3	7.0	12.9	0.7	17.2	15.9	0.8
DR2340	5.4	2.5	3.2	0.1	21.0	5.8	7.0	9.7	0.3	19.2	12.9	0.4
DR2180	5.2	4.7	6.0	0.2	21.4	3.9	6.0	5.7	0.2	18.4	11.7	0.4
DR2000	7.3	31.8	19.7	0.9	30.3	4.0	31.4	10.8	0.5	28.0	30.5	1.3
DR1900	10.1	10.9	22.8	0.4	23.5	4.7	9.7	9.5	0.2	19.6	32.2	0.5
DR1820	11.4	NA	19.9	0.4	NA	5.6	3.5	8.6	0.2	NA	28.5	0.6
DR1750	10.4	7.2	24.4	0.5	24.1	6.2	4.7	9.4	0.2	NA	33.8	0.6

Table 8: MAOM and DOC fractions

| Location | Silt & clay fraction / MAOM | | | | | DOC | |
	Mass	SOC concentration	Contribution of fractions to total SOC	SOC stock	C/N ratio	SOC stock	C/N ratio
	[g]	[%C]	[%C]	[kg C m^{-2}]	-	[g C m^{-2}]	-
IB2800	12.0	NA	NA	NA	NA	NA	2.5
IB2750	14.5	5.1	62.1	0.3	23.5	4.6	1.2
IB2570	18.1	10.7	59.0	0.9	10.5	8.5	1.2
IB2340	17.8	15.0	81.3	1.6	13.6	3.6	2.1
IB2180	18.2	15.8	70.4	1.6	15.8	6.6	5.2
IB2000	19.0	13.6	87.3	1.7	NA	11.3	1.8
IB1970	18.0	27.7	55.6	1.1	24.5	8.8	19.8
IB1840	16.2	17.1	61.7	1.2	16.6	2.3	6.1
FS3100	5.1	3.6	71.5	0.1	11.9	4.2	23.1
FS3040	3.9	3.9	66.8	0.1	10.9	5.4	18.3
FS2880	4.6	3.0	NA	NA	11.4	18.6	24.8
FS2800	6.2	1.3	68.4	NA	11.0	NA	10.3
FS2690	9.0	10.2	78.6	0.9	14.3	5.4	5.5
FS2630	13.4	NA	75.7	1.3	NA	16.2	1.8
FS2520	13.3	NA	70.1	1.6	NA	10.3	2.3
FS2320	9.6	17.7	60.4	1.0	14.1	9.9	8.9
FS2200	11.3	16.0	62.3	1.4	20.6	17.6	15.0
FS2000	10.1	17.0	NA	NA	13.1	7.5	7.3
FS1830	9.9	9.4	60.3	0.9	NA	12.0	7.5
DR2780	11.8	3.9	83.5	0.6	13.1	11.5	7.4
DR2690	14.2	NA	NA	NA	NA	5.1	13.7
DR2520	15.7	NA	84.1	4.4	NA	30.6	33.4
DR2340	16.4	21.9	87.1	2.7	14.7	17.7	14.1
DR2180	19.5	18.6	88.3	2.7	13.6	24.3	22.6
DR2000	17.7	NA	69.5	3.0	24.7	15.3	13.7
DR1900	14.7	22.4	67.8	1.2	15.6	5.8	15.0
DR1820	11.0	14.7	71.5	1.5	11.1	7.8	8.0
DR1750	11.3	17.9	66.2	1.3	22.7	13.3	28.5

8.2.4 Further statistics

*Table 9: Results of the linear mixed effects model testing the statistical significance of elevation, **parent material type (siliceous or calcareous, named Bedrock)**, and monthly variations on response variables. Bold values are p < 0.05. Note that not all residuals are normally distributed. Collums marked with * indicate a non-normal distribution of the residuals*

		Exposition		Slope*		pH*		SOC		C/N*		Soil temperature*		Fine earth moisture*		Volumetric soil moisture*		SR		SR$_{10}$*	
	Statistic	F	p	F	p	F	p	F	p	F	p	F	p	F	p	F	p	F	p	F	p
All sites	Elevation	0.87	0.98	1.975	0.91	4.291	0.658	9.516	0.911	26.81	**<0.01**	2.75	0.11	20.77	**<0.01**	1.39	0.25	12.67	**<0.01**	18.62	**<0.01**
	Bedrock	8.62	0.88	0.409	0.931	13.63	0.59	0.00	0.996	12.88	**<0.01**	0.09	0.76	0.17	0.69	0.07	0.80	11.54	**<0.01**	11.14	**<0.01**
	Month											6.77	**<0.01**	0.46	0.63	1.57	0.22	0.65	0.53		
	Elevation*Bedrock	4.75	0.95	0.261	0.942	0.081	0.898	0.031	0.976	9.72	**<0.01**	0.04	0.85	0.20	0.66	0.04	0.84	7.85	**0.01**	7.22	**0.01**
	Elevation*Month											16.76	**<0.01**	0.29	0.75	0.91	0.41	0.49	0.62		
	Bedrock*Month											0.55	0.58	2.62	0.08	1.97	0.15	0.77	0.47		
	Elevation*Bedrock*Month											0.34	0.72	1.94	0.16	1.62	0.21	0.37	0.70		

		Exposition*		Slope*		pH*		SOC*		C/N*		Soil temperature		Fine earth moisture		Volumetric soil moisture*		SR		SR$_{10}$*	
	Statistic	F	p	F	p	F	p	F	p	F	p	F	p	F	p	F	p	F	p	F	p
Sites above treeline	Elevation	0.45	0.96	16.25	0.86	308.70	**0.02**	26.09	0.61	33.69	**<0.01**	7.50	**0.01**	17.69	**0.01**	16.43	**0.01**	7.07	**0.02**	5.96	**0.03**
	Bedrock	11.79	0.92	2.66	0.98	10.79	0.17	2.82	0.81	19.21	**<0.01**	0.54	0.47	0.61	0.45	1.85	0.19	7.81	**0.01**	3.50	0.08
	Month											3.22	0.05	0.08	0.92	0.28	0.76	1.65	0.21		
	Elevation*Bedrock	6.86	0.93	1.87	0.99	5.83	0.22	1.63	0.75	10.54	**<0.01**	0.46	0.51	0.59	0.45	1.38	0.26	6.21	**0.02**	2.44	0.14
	Elevation*Month											7.84	**<0.01**	0.10	0.91	0.13	0.88	0.95	0.40		
	Bedrock*Month											0.91	0.41	0.17	0.85	1.65	0.21	2.94	0.07		
	Elevation*Bedrock*Month											0.66	0.52	0.28	0.76	1.43	0.25	2.35	0.12		

Table 10: Results of the linear mixed effects model testing the statistical significance of elevation and **parent material type (siliceous or calcareous, named Bedrock)**, on response variables within the soil fractions for the entire transect length. Bold values are p < 0.05. Note that not all residuals are normally distributed. Collums marked with * indicate a non-normal distribution of the residuals. The third table row shows the results of the soil fractionation model where the effects of elevation, bedrock type, and fraction on response variables have been investigated

	Coarse sand fraction / cPOM										Fine sand fraction / fPOM									
	Mass*		SOC concentration*		Contribution of cPOM to total SOC*		SOC stock *		C/N ratio*		Mass*		SOC concentration*		Contribution of fPOM to total SOC*		SOC stock		C/N ratio*	
Statistic	F	p	F	p	F	p	F	p	F	p	F	p	F	p	F	p	F	p	F	p
Elevation	6.71	0.93	12.70	0.63	3.48	0.33	4.45	**0.05**	4.43	0.65	22.80	0.29	5.82	**0.03**	2.58	0.53	1.73	0.20	42.60	1.00
Bedrock	0.06	0.97	0.56	0.80	0.20	0.74	0.42	0.52	0.09	0.92	3.61	0.46	1.16	0.29	2.99	0.52	0.09	0.77	4.04	1.00
Elevation*Bedrock	2.28	0.94	0.27	0.85	0.20	0.74	0.35	0.56	0.21	0.82	4.85	0.43	0.92	0.35	4.46	0.48	0.11	0.74	2.12	1.00

	cPOM + fPOM				Silt & clay fraction / MAOM										DOC			
	Contribution of fractions to total SOC*		SOC stock *		Mass*		SOC concentration*		Contribution of MAOM to total SOC*		SOC stock*		C/N ratio*		SOC stock*		C/N ratio*	
Statistic	F	p	F	p	F	p	F	p	F	p	F	p	F	p	F	p	F	p
Elevation	0.13	1.00	20.45	**0.01**	10.41	0.99	54.86	1.00	0.00	1.00	13.48	**<0.01**	4.53	**0.04**	0.39	0.97	42.60	1.00
Bedrock	0.91	1.00	0.47	0.53	0.24	0.99	0.34	1.00	1.41	0.84	0.20	0.66	0.73	0.40	0.56	0.97	4.04	1.00
Elevation*Bedrock	1.56	1.00	0.35	0.59	0.07	1.00	0.22	1.00	2.03	0.83	0.06	0.81	1.27	0.27	0.03	0.99	2.12	1.00

	cPOM + fPOM + MAOM									
	Mass		SOC concentration		Contribution of fractions to total SOC*		SOC stock*		C/N ratio	
Statistic	F	p	F	p	F	p	F	p	F	p
Elevation	0.00	0.95	12.05	**<0.01**	0.02	0.90	2.82	0.11	16.83	**<0.01**
Bedrock	0.00	0.98	0.82	0.37	0.02	0.90	0.04	0.85	2.08	0.16
Fraction	11.82	**<0.01**	3.52	**0.04**	6.27	**<0.01**	3.06	0.06	8.52	**<0.01**
Elevation*Bedrock	0.01	0.93	0.60	0.45	0.02	0.89	0.00	0.95	1.41	0.25
Elevation*Fraction	5.80	**<0.01**	1.52	0.24	0.67	0.52	1.04	0.36	6.07	**<0.01**
Bedrock*Fraction	0.18	0.84	1.26	0.30	0.61	0.55	0.01	0.99	2.74	0.09
Elevation*Bedrock*Fraction	0.62	0.54	0.60	0.56	0.88	0.42	0.04	0.96	2.29	0.12

8.2.5 List of figures

8.2.6   List of tables

Personal declaration:

I hereby declare that the material contained in this thesis is my own original work. Any quotation or paraphrase in this thesis from the published or unpublished work of another individual or institution has been duly acknowledged. I have not submitted this thesis, or any part of it, previously to any institution for assessment purposes.

Zurich, 26.04.2024

Cédric Bührer